RESEARCH ARTICLE



Check for updates

Primate body mass and dietary correlates of tooth root surface area

Ashley R. Deutsch¹ | Edwin Dickinson¹ | Victoria A. Whichard¹ | Giulia R. Lagomarsino¹ | Jonathan M. G. Perry² | Kornelius Kupczik^{3,4} | Adam Hartstone-Rose¹ |

Correspondence

Ashley R. Deutsch, Department of Biological Sciences, North Carolina State University, Raleigh, NC, USA. Email: adeutsc@ncsu.edu

Funding information

LSB Leakey Foundation; NYCEP; Stony Brook University; Duke University, Grant/Award Numbers: DBI-1902242, DBI-192242; National Science Foundation, Grant/Award Numbers: BCS-01000825, DDIG #0925793, BCS-0851272, BCS-0090255, BCS 1540421, IOS-15-57125, ECCS-2025064

Abstract

Objectives: This study aims to examine primate postcanine tooth root surface area (TRSA) in the context of two ecological variables (diet and bite force). We also assess scaling relationships within distinct taxonomic groups and across the order as a whole.

Materials and Methods: Mandibular postcanine TRSA was measured using a three-dimensional computed tomography (CT) method for catarrhine (N=27), platyrrhine (N=21), and strepsirrhine (N=24) taxa; this represents the first sample of strepsirrhines. Two different body size proxies were used: cranial geometric mean (GM) using nine linear measurements, and literature-derived body mass (BM).

Results: TRSA correlated strongly with body size, scaling with positive allometry or isometry across the order as a whole; however, scaling differed significantly between taxa for some teeth. Among Strepsirrhini, molar TRSA relative to GM differed significantly between folivores and pliant-object feeders. Additionally, P_4 TRSA relative to BM differentiated folivores from both hard- and pliant-object feeders. Among Cercopithecoidea, P_4 TRSA adjusted by GM differed between hard- and pliant-object feeders.

Discussion: Dietary signals in TRSA appear primarily driven by high frequency loading experienced by folivores. Stronger and more frequent dietary signals were observed within Strepsirrhini relative to Haplorhini. This may reflect the constraints of orthognathism within the latter, constraining the adaptability of their postcanine teeth. Finally, because of the strong correlation between TRSA and BM for each tooth locus (mean $r^2 = 0.82$), TRSA can be used to predict BM in fossil primates using provided equations.

KEYWORDS

allometry, Catarrhini, Hominoidea, Platyrrhini, Strepsirrhini

1 | INTRODUCTION

Primate dentition acts in conjunction with the myological and osteological components of the masticatory apparatus to mechanically process foods. As such, the functional demands of diet have shaped dental morphology throughout evolutionary history. While tooth crown morphology has been shown to correlate with diet in primates (e.g., Kay, 1975, 1978; Rosenberger & Kinzey, 1976; Winchester

¹Department of Biological Sciences, North Carolina State University, Raleigh, North Carolina, USA

²Department of Physical Therapy Education, Western University of Health Sciences, Lebanon, Oregon, USA

³Department of Human Evolution, Max Planck Institute for Evolutionary Anthropology, Leipzig, Germany

⁴Department of Anthropology, University of Chile, Santiago, Chile

et al., 2014), it is also likely that tooth root morphology has been adaptively shaped by masticatory loading environments and may reflect dietary specialization (Kupczik & Dean, 2008; Perry et al., 2010; Spencer, 2003). Within this study, we provide tooth root surface area (TRSA) measures produced using computed tomography (CT) data for a large and diverse primate sample to examine the relationship between TRSA and several ecomorphological correlates in extant primates. In doing so, we analyze the relationship between TRSA and bite force (BF), as well as between TRSA and dietary category. BFs are anatomically derived and measured following Deutsch et al. (2020). This research expands upon previous work within Catarrhini and Platyrrhini (Kupczik, 2003; Perry et al., 2010; Spencer, 2003) and, for the first time, presents data for Strepsirrhini. Understanding dietary signals in TRSA may have utility for reconstructing diet in fossil species, particularly for fragmentary material where tooth crowns are unavailable. The examination of the relationship between TRSA and diet within this most complete primate sample to date, made possible through advancements in CT technology, will allow for broader applicability of TRSA in dietary inference of fossil primates.

1.1 | The primate masticatory apparatus

The jaw adductor musculature in primates is comprised of the temporalis, masseter, and medial pterygoid muscles. These muscles act together to generate masticatory forces. Whereas the intrinsic architecture of the masticatory adductors drives muscle force production (Gans & Bock, 1965; Hartstone-Rose et al., 2018; Lieber & Fridén, 2000; Lieber & Ward, 2011), the mechanical efficiency of force transfer from these muscles to a bite along the tooth row is impacted by the biomechanical configuration of both the dentition and the muscle attachments (Deutsch et al., 2020; Greaves, 1978, 1983, 2012; Radinsky, 1981; Spencer, 1999). As such, the masticatory musculature and the craniomandibular morphology together contribute to masticatory performance. Although bite leverage allows for larger potential forces at posterior bite points, this force increase occurs at the expense of linear gape potential. This trade off leads to functional distinctions between teeth along the tooth row (Perry et al., 2010; Spencer, 1998; Perry, Hartstone-Rose, & Wall, 2011), resulting in differences in loading environments experienced by different teeth.

During masticatory loading, BFs produced by the masticatory apparatus are applied to the teeth at the crowns then transmitted through the tooth roots and the periodontal ligament into the alveolar bone. These forces have the potential to dislodge a tooth from the alveolus; however, the periodontal ligament secures the cementum of the tooth roots to the alveolar bone with a meshwork of Sharpey's fibers (Beertsen et al., 1997). This ligament surrounds the root surface and plays an important role in anchoring the tooth and dissipating masticatory forces. A greater TRSA is theoretically capable of accommodating a larger periodontal ligament composed of more or thicker Sharpey's fibers. It has therefore been previously predicted that TRSA will reflect dietary mechanical properties, such that species that

consume more mechanically challenging diets and thus require larger or more repetitive forces will have larger TRSAs than those that consume softer diets in order to resist tooth displacement (Kovacs, 1971, 1979; Kupczik, 2003; Kupczik & Dean, 2008; Perry et al., 2010; Spencer, 1998).

While there exists a theoretical relationship between BF and dietary category (Eng et al., 2009; Perry, 2018; Perry, Hartstone-Rose, & Wall, 2011; Taylor & Vinyard, 2009), in that species that consume mechanically challenging diets must habitually produce larger or more frequent BFs, previous literature does not reflect this relationship independent of body size. Dietary signals have been absent in both physiological cross-sectional area (PCSA)-a myological correlate of a muscle's force potential (Anapol et al., 2008; Close, 1972; Gans, 1982; Hartstone-Rose et al., 2018; Lieber, 1986; Schumacher, 1961)--and anatomically derived BF (the combination of that myological force with osteological leverage), which instead scales with pure allometry (Deutsch et al., 2020; Perry, Hartstone-Rose, & Logan, 2011). This puzzling finding is likely due to the nature of anatomically derived BF. which is calculated as the summed PCSA of the jaw adductor muscles, and therefore estimates the maximal force which can be generated when all muscles are firing maximally and simultaneously. This is an unrealistic and potentially impossible behavior—for example, we know the masticatory adductors fire at different times during the chewing cycle (e.g., Hylander et al., 1987; Vinyard et al., 2008) and muscle architecture, including PCSA, and therefore the capacity for force generation varies within a given gape cycle and across gape cycles of different velocity (Laird et al., 2020)-but the assumption of maximal contraction is necessary in the absence of sufficient in vivo data, as no direct evidence exists for what percentage of the muscle is being used in any given bite for the vast majority of taxa. In rodent models. habitual BF has been found to be lower than BF predicted based on PCSA (Becerra et al., 2011); thus, it is likely that within primates, myological estimates of BF potential also overestimate actual BFs.

1.2 | Body size and dietary correlates in nonprimate lineages

TRSA has been quantified in the context of dietary ecology and BF in a number of non-primate mammalian lineages, including Carnivora and Chiroptera. Across four similarly-sized phyllostomid bats occupying a range of dietary niches, food hardness proved an important ecological variable driving TRSA (Self, 2015). Specifically, insectivorous taxa (Mimon bennettii and Macrotus californicus) and a seed processing frugivore (Carollia villosum) demonstrated significantly greater TRSAs than the frugivorous Carollia perspicillata, despite the close phylogenetic relationship of the latter two taxa. BF, estimated anatomically using osteological measurements, also correlated strongly with TRSA (Self, 2015). A similar dietary relationship can be observed among Carnivorans. Across 21 species from four families (Canidae, Felidae, Ursidae, and Hyaenidae), taxa that habitually consumed mechanically hard food items demonstrated significantly greater TRSA than species consuming soft or tough foods (Kupczik & Stynder, 2012).

Additionally, the authors observed a relationship between TRSA and prey size, such that carnivores that hunt and consume relatively larger prey showed an increase in TRSA (Kupczik & Stynder, 2012). Thus, adaptability in TRSA can be seen in response to shifts in diet across diverse phylogenies, with increasing magnitudes of mechanical loading being associated with a corresponding shift in increasing TRSA.

1.3 | Dietary correlates of TRSA within primates

While tooth crown morphology has been studied extensively in relation to diet within the primate order (e.g., Kay, 1975, 1978; Rosenberger & Kinzey, 1976; Winchester et al., 2014), fewer studies have examined the relationship between tooth root morphology and masticatory performance. Much of this literature has assessed tooth root morphology within Hominidae (e.g., Kupczik, 2003; Kupczik & Dean, 2008; Kupczik & Hublin, 2010; Wood et al., 1988); however, few studies have assessed the relationship between TRSA and diet within Cercopithecoidea and Platyrrhini.

Within Catarrhini the relationship between TRSA and diet has been assessed in a few extant taxa (*Homo sapiens*, *Gorilla gorilla*, *Pongo pygmaeus*, *Pan troglodytes*, and *Papio anubis*; Kupczik, 2003). Among the hominoids within this sample, the highly frugivorous *P. troglodytes* was found to have the smallest TRSA among the hominoids within the sample, while *G. gorilla*, which consumes a particularly folivorous diet among apes (Remis et al., 2001), was found to have the largest relative total postcanine TRSA (Kupczik, 2003). M_2 root surface area has also been examined relative to crown surface area in a larger catarrhine sample (n=58; Kupczik et al., 2009). While this study observed a strong phylogenetic signal, root surface area was larger relative to crown surface area in hard-object feeders when compared to soft or tough object feeders.

Similar correlations between dietary category and TRSA have been reported within Platyrrhini. Spencer (2003), using a two-dimensional projection method, and Perry et al. (2010), using a three-dimensional CT method, found that species that consume harder or tougher diets (i.e., hard seeds or leaves) had larger TRSAs relative to body size than do those that consume softer diets. These dietary patterns in TRSA found in extant species have been applied to taxonomically related extinct species in order to infer diet (Kupczik & Dean, 2008; Perry et al., 2010).

The observed relationship between TRSA and diet relates to variation in mechanical properties and, therefore, BFs produced during mastication. TRSA, however, must resist actual BFs rather than theoretical maximal BFs. As such, TRSA may be poorly correlated with anatomically derived BF. TRSA should, however, scale better than anatomically derived BF with dietary categories as well as in vivo BFs. This indirect, non-myological approach may resolve issues with BF estimation and produce better signals for functional masticatory performance. Alternatively, examining the relationship between these masticatory performance variables in an expanded sample of primates may help to clarify the BF signal and resolve the missing causal relationship.

2 | AIMS AND PREDICTIONS

This study aims to examine the correlation between body size adjusted postcanine mandibular TRSA and masticatory performance (diet and anatomically derived BFs) across the most taxonomically diverse and largest sample of primates heretofore examined for these variables. The data presented expand current understanding of correlates of TRSA within catarrhines and platyrrhines and for the first time, present TRSA data for strepsirrhines. We assess previously reported correlations between TRSA and dietary category (Kupczik, 2003; Perry et al., 2010; Spencer, 2003) across the order as a whole. This study also examines the correlation between TRSA and anatomically derived maximal BF through the incorporation of previously published BF estimates (Hartstone-Rose et al., 2018; Perry et al., 2010, 2014; Perry, Hartstone-Rose, & Logan, 2011) as well as novel BF calculations for five additional taxa and investigates TRSA scaling. These observations are contextualized within the order Primates as a whole and within individual major primate subdivisions (Strepsirrhini, Platvrrhini, Cercopithecoidea, and Hominoidea).

2.1 | Prediction 1. TRSA will scale with positive allometry relative to body size across the order Primates and within each lineage

Previous studies of scaling relationships of other force-related masticatory variables within primates have largely reported findings of positive allometry relative to body size. Among hominoids, PCSA has also been found to scale with positive allometry relative to jaw length and condyle-molar length (Taylor & Vinyard, 2013). Within both platyrrhines and cercopithecoids, anatomically derived BF was found to scale with positive allometry relative to cranial geometric mean (GM) (Deutsch et al., 2020), as were some measures of muscle mass and PCSA (Hartstone-Rose et al., 2018). Alternatively, TRSA may scale with isometry. Within platyrrhines and cercopithecoids, some measures of adductor muscle mass and PCSA have been found to scale with isometry (Hartstone-Rose et al., 2018) as has PCSA within strepsirrhines (Perry, Hartstone-Rose, & Wall, 2011).

2.2 | Prediction 2. Species that consume obdurate diets, such as hard seeds and tough foliage, will have larger TRSAs than do those that consume soft diets

While processing hard foods requires high magnitude forces, processing tough foods requires high frequency forces. As such, the teeth of species that consume a mechanically challenging diet experience larger or more frequent forces. TRSA may be larger to accommodate a larger periodontal ligament and resist displacement. A relationship between TRSA and diet has been found within hominoids as well as in small samples of cercopithecoids and platyrrhines (Kupczik, 2003; Perry et al., 2010; Spencer, 2003). This study will assess whether similar trends are observed across the entire order. Alternatively, TRSA may scale with a purely allometric signal, as has been observed previously in PCSA and BF (Deutsch et al., 2020; Hartstone-Rose et al., 2018; Perry, Hartstone-Rose, &

Logan, 2011) in which case TRSA should not correlate better with diet than with body size across the order as a whole.

2.3 | Prediction 3. Body size adjusted TRSA and dietary category will be similarly correlated across all primate lineages

If the mechanical properties of diet primarily drive variation in tooth root morphology, TRSA should correlate similarly across all lineages. Alternatively, taxonomic variation may shape or constrain TRSA differently between lineages. For instance, among haplorhines, incisors are regularly utilized for ingestion, while postcanine teeth are involved in mastication (Hiiemae & Kay, 1972; Rosenberger, 1992). Tooth-combed strepsirrhines, however, rarely utilize anterior dentition for ingestion. Instead, strepsirrhines tend to ingest food using premolars (Hiiemae & Kay, 1972; Perry, 2008; Perry & Hartstone-Rose, 2010; Yamashita, 2003). Therefore, the loading environment of strepsirrhine premolars differs from that of haplorhine premolars. This functional difference, or the phylogenetic differences themselves, may be reflected in root morphology.

2.4 | Prediction 4. Body size adjusted TRSA will be similarly correlated with dietary category across all postcanine teeth

If TRSA is correlated with forceful chewing alone, surface area will scale similarly with actual BF across all teeth. Alternatively, other factors such as craniofacial height, which influence root morphology (Cobb & Baverstock, 2009), may independently shape TRSA and unevenly obscure masticatory signals across different teeth, such that some tooth loci are more tightly correlated with function than are others.

2.5 | Prediction 5. Anatomically derived BFs will not correlate highly with TRSA

Within primates, anatomically derived BF has been found to scale with pure allometry rather than correlate with dietary category (Deutsch et al., 2020; Perry, Hartstone-Rose, & Logan, 2011). If BF estimates do not reflect habitual BFs, TRSA should correlate more with diet than anatomically derived BF. Alternatively, however, given that tooth placement within the jaw has a direct biomechanical relationship with leverage, tooth roots my correlate more with BF than has previously been observed for other variables.

3 | MATERIALS AND METHODS

3.1 | Sample

This sample includes 75 primate specimens (9 hominoids, 20 cercopithecoids, 21 platyrrhines, 1 tarsiiform, and 24 strepsirrhines)

representing 51 genera and 73 species (Table 1). Osteological specimens included in this study are both wild- and captive-raised individuals. As such, this study does not account for potential impacts of captivity on body size or morphology (see Leigh, 1994 and Siciliano-Martina et al., 2021 for examples of the effects of captivity on primates). Mandibular postcanine TRSA measurements were taken of all postcanine teeth, regardless of dental formula, along a hemi-mandible for each specimen. Handling of dental formula variation across the sample is discussed in greater detail below. For a subsample (n = 50), these measures were combined with novel leverage measurements and previously reported PCSA data from Perry and Wall (2008), Perry, Hartstone-Rose, and Wall (2011), Perry et al. (2014), and Hartstone-Rose et al. (2018), as well as novel PCSA measurements for five additional taxa. Bite leverage and TRSA were measured from CT scans of skulls of conspecifics. These scans were newly produced at the Shared Materials Instrumentation Facility (SMIF) at Duke University or downloaded from MorphoSource (Boyer et al., 2016) and the Kyoto University Primate Research Institute's (KUPRI) Digital Morphology Museum databases (see specific attributions in Table 1). For taxa with 10% or more body mass (BM) sexual dimorphism, conspecifics of the same sex as the previously published specimens were chosen for novel analyses. As such, each species was represented by a single set of PCSA values as well as a single set of bite leverage measurements and TRSA measurements, but these measurements were derived from two different specimens of the same species. This approach relies on the assumption that interspecific variation is larger than intraspecific variation—a clear but unavoidable limitation given the availability of necessary data.

3.2 | BF estimation

Anatomically derived BF was estimated for a subset of the total sample (n=50). For this sample, PCSA for each masticatory adductor group (masseter, temporalis, and medial pterygoid) was drawn from Perry and Wall (2008), Perry, Hartstone-Rose, and Wall (2011), Perry et al. (2014), and Hartstone-Rose et al. (2018) and calculated for five additional specimens according to a formula modified from Schumacher (1961):

$$q = m/lp$$

where q is PCSA, m is muscle mass, l is fascicle length, and p is a constant representing the specific density of mammalian masticatory muscle (1.0606 g/cm³; Leonard, Worden, Boettcher, Dickinson, Omstead, et al., 2021). For all preserved specimens (i.e., those not dissected fresh/frozen), muscle mass was multiplied by a correction factor to account for changes related to preservation based on Leonard, Worden, Boettcher, Dickinson, and Hartstone-Rose (2021a) and Leonard, Worden, Boettcher, Dickinson, and Hartstone-Rose (2021b). All museum specimens were assumed to have been subjected to long term storage (more than 30 days).

BFs were then calculated at the most mesiobuccal cusp of each postcanine tooth in the right mandibular quadrant (see Figure 1). To do this, each muscle's PCSA was translated to intrinsic muscle force using a constant for skeletal muscle force production (3 kg/cm²;

TABLE 1 Full list of analyzed specimens alongside body mass, cranial geometric mean, and dietary categorization

	Species	Sex	Dietary category	臣	BM (g) ^a	Specimen number	MorphoSource identifier	Media number
Hominoid	Hylobates Iar ^b	щ	Soft	5.07	2000	KUPRI 8134		1325 (cranium)
								1326 (mandible)
	Symphalangus syndactylus ^c	щ	Soft	5.74	10,300	amnh:mammals:m-102724	ark:/87602/m4/M26157	000026157
	Pongo abelii ^b	Σ	Soft	10.38	57,500	Baran (GAIN 8)		796 (cranium)
								797 (mandible)
	P. pygmaeus ^c	ш	Soft	8.77	37,500	mcz:mamm:37518	doi:10.17602/M2/M4613	000004613 (cranium)
							doi:10.1/602/M2/M4614	000004614 (mandible)
	Gorilla gorilla ^c	Σ	Folivore	12.13	168,000	amnh:mammals:m-167338	ark:/87602/m4/M21963 ark:/87602/m4/M21965	000021963 (cranium) 000021965 (mandible)
	G. gorilla ^c	щ	Folivore	9.7	92,000	amnh:mammals:m-54356	ark:/87602/m4/M21957	000021957
	Pan troglodytes ^c	Σ	Soft	10.76	49,000	amnh:mammals:m-167342	ark:/87602/m4/M21967	000021967
	P. troglodytes ^c	ш	Soft	8.4	35,000	mcz:mamm:17702	doi:10.17602/M2/M4395 doi:10.17602/M2/M4396	000004395 (cranium) 000004396 (mandible)
	P. paniscus ^c	ш	Soft	7.59	31,000	mcz:mamm:38019	doi:10.17602/M2/M4398	000004398
Cercopithecoid	Cercocebus torquatus ^{c,d}	ш	Hard	5.13	9200	mcz:mamm:18612	doi:10.17602/M2/M2599	000002599
	Cercopithecus campbelli ^{b,d}	ш	Soft	4.75	2200	KUPRI 986		1070 (cranium)
								1071 (mandible)
	C. cephus ^{c,d}	щ	Soft	4.54	3000	sbu:rs:85-11	ark:/87602/m4/M23539	000023539
	C. mona ^{b,d}	ш	Soft	4.38	3250	KUPRI 7296		969 (cranium)
								970 (mandible)
	C. neglectus ^{b,d}	Σ	Soft	5.21	2200	KUPRI 7121		971 (cranium)
								972 (mandible)
	C. petaurista ^{b,d}	ш	Folivore	4.02	2900	KUPRI 1007		1061 (cranium)
								1060 (mandible)
	Chlorocebus aethiops ^{c,d}	Σ	Folivore	4.76	3200	uta:z138	ark:/87602/m4/M162767	000162767
	Colobus guereza ^{c,d}	ш	Folivore	5.35	7850	anmh:mammals:m-52215	ark:/87602/m4/M12514	000012514
	Erythrocebus patas ^c	Σ	Soft	90.9	1,0000	anmh:mammals:m-34714	ark:/87602/m4/M16053	000016053
	Macaca silenus ^{b,d}	Σ	Soft	6.05	7500	KUPRI 6224		1134 (cranium)
								1133 (mandible)
	M. sylvanus ^{c,d}	Σ	Folivore	6.47	12,200	usnm:mammals:476780	ark:/87602/m4/M20357	000020357
	Mandrillus sphinx ^{c,d}	ш	Hard	6.82	12,000	mcz:mamm:34272	doi:10.17602/M2/M5099	000002036
	Miopithecus talapoin ^{c,d}	Σ	Soft	3.36	1250	mcz:mamm:23197	doi:10.17602/M2/M5093	000005093
	Nasalis Iarvatus	Σ	Folivore	5.95	22,000	AHR 103040	ark:/87602/m4/388859	000388859

TABLE 1 (Continued)

	Species	Şex	Dietary category	Σ	BM (g) _a	Specimen number	MorphoSource identifier	Media number
	Papio anubis ^c	Σ	Soft	9.01	26,000	amnh:mammals:m-52677	ark:/87602/m4/M13624	000013624
	Presbytis rubicunda ^c	Σ	Folivore	4.85	9200	anmh:mammals:m-103637	ark:/87602/m4/M18343	000018343
	Procolobus verus ^c	Σ	Folivore	6.31	4850	anmh:mammals:m-89439	ark:/87602/m4/M18331	000018331
	Semnopithecus entellus ^c	ш	Folivore	5.27	12,800	anmh:mammals:m-90328	ark:/87602/m4/M14456	000014456
	Theropithecus gelada $^{ ext{c}}$	Σ	Folivore	68.9	25,000	anmh:mammals:m-60568	ark:/87602/m4/M13673	000013673
	Trachypithecus cristatus ^c	ш	Folivore	4.64	5700	mcz:mammals:35586	doi:10.17602/M2/M4435	000004435
Platyrrhine	Alouatta guariba ^c	ш	Folivore	5.01	4550	usnm:mammals:518255	ark:/87602/m4/M114305	000114305
	A. palliata ^c	×	Folivore	5.29	9020	usnm:mammals:11393	doi:10.17602/M2/M13169	000013169
	Aotus nancymae ^{d,e}	Σ	Insectivore	3.04	794.5	AHR 106001	ark:/87602/m4/388890	000388890
	Ateles geoffroyi ^c	ш	Soft	5.18	7225	usnm:mammals:291056	doi:10.17602/M2/M13043	000013043
	Brachyteles arachnoides ^b	×	Folivore	5.53	9350	KUPRI 4690		544 (cranium)
								545 (mandible)
	Cacajao melanocephalus ^c	ш	Hard	4.52	2700	usnm:mammals:256217	ark:/87602/m4/M114310	000114310
	Callicebus torquatus ^c	щ	Soft	3.44	1250	usmn:mammals:406411	ark:/87602/m4/M114311	000114311
	Callimico goeldii	Σ	Soft	2.69	366	usnm:mammals:464993	ark:/87602/m4/M115841	000115841
	Callithrix jacchus ^{d,e}	Σ	Soft	2.26	317.9	AHR 108035	ark:/87602/m4/388911	000388911
	C. pygmaea	Σ	Soft	1.69	112.5	AHR 108002	ark:/87602/m4/388926	000388926
	Cebus olivaceus ^c	щ	Soft	4.35	2650	Usnm:mammals:338960	ark:/87602/m4/M114320	000114320
	Chiropotes sagulatus ^{c,d}	Σ	Hard	4.81	3250	usnm:mammals:338964	doi:10.17602/M2/M13229	000013229
	Leontopithecus rosalia	Σ	Soft	2.66	710	AHR 108006	ark:/87602/m4/388931	000388931
	Mico argentatus ^{c,d}	Σ	Soft	2.09	349	mcz:mamm:30580	doi:10.17602/M2/M5193	000005193
	Pithecia pithecia ^c	Σ	Hard	3.66	1550	usnm:mammals:339658	doi:10.17602/M2/M13349	000013349
	Saguinus bicolor	ш	Soft	2.52	540	AHR 108004	ark:/87602/m4/388955	000388955
	S. Iabiatus ^{d,e}	ш	Soft	2.44	455	AHR 108001	ark:/87602/m4/388974	000388974
	S. midas	щ	Insectivore	2.54	440	AHR 108021	ark:/87602/m4/389189	000389189
	S. oedipus ^{d,e}	щ	Soft	2.32	404.1	AHR 108005	ark:/87602/m4/389183	000389183
	Saimiri sciureus ^{c,d}	щ	Soft	2.77	875	mcz:mamm:30568	doi:10.17602/M2/M4483	000004483
	Sapajus apella ^{c,d}	ш	Hard	4.06	2350	mcz:mamm:30726	doi:10.17602/M2/M5211	000005211
Tarsier	Tarsius syrichta ^{c,f}	×	Insectivore	2.15	128.5	dlc:50m	ark:/87602/m4/M158814	000158814
	Avahi laniger ^{c.8}	×	Folivore	2.54	1200	mcz:mamm:44877	doi:10.17602/M2/M2731	000002731
	Cheirogaleus medius ^{e,8}	×	Soft	2.1	135	AHR 116004	ark:/87602/m4/389000	000389000
	Daubentonia madagascariensis ^{e,h}	×	Soft	4.68	2500	AHR 112001	ark:/87602/m4/385050	000385050

Media number	000002670
MorphoSource identifier	doi:10.17602/M2/M2670
Specimen number	mcz:mamm:44887
BM (g) ^a	2200
Æ	3.66
Dietary category	Soft
Şex	×
Species	Eulemur collaris ^{c.8}

(Continued)

TABLE 1

number	929	990	052	851	589	039	020	950	.664	049	023	028	719	831	029	038	459	033	044	726	700
Media number	000002670	000385065	000388052	000014851	000002685	000385039	000385020	000013038	000011664	000389049	000389023	000389028	000002719	000028831	000385029	000389038	000165459	000389033	000389044	000002726	000385007
urce	doi:10.17602/M2/M2670	ark:/87602/m4/385065	ark:/87602/m4/388055	doi:10.17602/M2/M14851	doi:10.17602/M2/M2685	ark:/87602/m4/385039	ark:/87602/m4/385020	doi:10.17602/M2/M13038	doi:10.17602/M2/M11664	ark:/87602/m4/389049	ark:/87602/m4/389023	ark:/87602/m4/389028	doi:10.17602/M2/M2719	doi:10.17602/M2/M28831	ark:/87602/m4/385029	ark:/87602/m4/389038	ark:/87602/m4/M165459	ark:/87602/m4/389033	ark:/87602/m4/389044	doi:10.17602/M2/M2726	25/1./07402/m//205007
MorphoSource identifier	doi:10.176	ark:/87602	ark:/87602	doi:10.176	doi:10.176	ark:/87602	ark:/87602	doi:10.176	doi:10.176	ark:/87602	ark:/87602	ark:/87602	doi:10.176	doi:10.176	ark:/87602	ark:/87602	ark:/87602	ark:/87602	ark:/87602	doi:10.176	70760/://
umber	:44887	35	82		:16075	11	12	anmh:mammals:m-170561	amnh:mammals:m-170568	CNR:Herrel lab:893AAJ	70	33	36035		1	11		60	1	:44854	5
Specimen number	mcz:mamm:44887	AHR 114035	AHR 114038	dlc:2041m	mcz:mamm:16075	AHR 114021	AHR 114042	anmh:mamr	amnh:mamr	CNR:Herrel	AHR 116007	AHR 110003	mcz:mamm:36035	du:ea:194	AHR 111021	AHR 110001	dlc:6841m	AHR 113009	AHR 113011	Mcz:mamm:44854	ALID 44 40 44
BM (g) ^a	2200	1300	1200	175	225	813	2200	280	1000	09	308	742.5	424	1400	822.5	925	3700	6250	3500	2900	0000
Σ	3.66	3.55	3.39	1.99	1.93	3.16	3.6	2.23	2.23	1.45	2.17	2.76	2.35	2.89	3.04	3.44	4.33	3.81	4.07	3.98	00.7
Dietary category	Soft	Soft	Soft	Insectivore	Soft	Folivore	Folivore	Folivore	Folivore	Insectivore	Soft	Soft	Soft	Insectivore	Hard	Soft	Folivore	Folivore	Hard	Folivore	400
Sex	×	×	×	×	×	×	×	×	×	×	×	×	×	×	×	×	×	×	×	×	>
Species	Eulemur collaris ^{c,g}	E. coronatus ^{e,g}	E. mongoz ^{e, g}	Galago moholi ^{c.g}	G. senegalensis ^{e, g}	Hapalemur griseus ^{e.g}	Lemur catta ^{e,g}	Lepilemur leucopus ^{c.8}	L. mustelinus	Microcebus murinus ^{e,g}	Mirza coquereli ^{e,g}	Nycticebus coucang ^{e,g}	N. pygmaeus ^{c.g}	Otolemur crassicaudatus ^{c,g}	O. garnettii ^{e,g}	Perodicticus potto ^{e,g}	Propithecus coquereli ^{c, g}	P. diadema ^{e,g}	P. tattersalli ^{e,g}	P. verreauxi ^{c,f}	9.000
					Strepsirrhine																

Abbreviations: BM, body mass; GM, geometric mean; PCSA, physiological cross-sectional area.

^aBody mass from species average for sex listed in Mittermeier et al. (2012). For individuals of unknown sex, species average was used.

^bScans downloaded from Kyoto University Primate Research Institute's (KUPRI) Digital Morphology Museum database.

^cScans downloaded from MorphoSource.org, Duke University.

^dPCSA data from Hartstone-Rose et al. (2018).

^eScans produced at the Shared Materials Instrumentation Facility (SMIF) at Duke University.

^fPCSA data from Perry and Wall (2008).

⁸PCSA data from Perry, Hartstone-Rose, and Logan (2011).

^hPCSA data from Perry et al. (2014).

Close, 1972). Muscle mechanical advantage was calculated following Hartstone-Rose et al. (2018) from lateral photographs of each skull in occlusion. These images were taken from three-dimensional renderings of skull surfaces employing the "non-perspective" setting. Muscle origin and insertion areas for each group were outlined to compute the centroid of each muscle's attachment sites using ImageJ (Rueden et al., 2017). Bony prominences viewed in the lateral photographs were used as markers to identify the origin and insertion of each muscle in each specimen. Each muscle's line of action was then drawn connecting the centroid of the muscle's origin to the centroid of the muscle's insertion. Lever arm lengths were then measured as the distance between each muscle's line of action and the center of rotation on the mandibular condyle (fulcrum of the temporomandibular joint) perpendicular to the line of action. While the mandible does not rotate purely around a single point (Terhune et al., 2011), free body diagrams can be performed around any axis of rotation. The chosen point can be reliably marked and has been used in previous studies of mastication (Deutsch et al., 2020: Hartstone-Rose et al., 2012). Load arms were measured as the distances from the center of rotation on the condyle to several chosen bite points. In order to account for the effort on both the working-side and balancing-side of the jaw, the moment arm of the balancing side of the system was modeled as the distance from the point of rotation on the mandibular condyle to the infradentale plus the distance from the infradentale back to the bite point following Hartstone-Rose et al. (2012) and Deutsch et al. (2020). This measurement assumed bilateral symmetry of the specimens and maximal contraction of bilateral mandibular adductors. To calculate total BF. these measurements were combined, following Hartstone-Rose et al. (2012), (2019), Deutsch et al. (2020), and Hartstone-Rose et al. (2021) using the formula:

$$\mathsf{BF_D} = c \bigg(\frac{(q_{\mathsf{MS}} \mathsf{L}_{\mathsf{MS}}) + (q_{\mathsf{TMP}} \mathsf{L}_{\mathsf{TMP}}) + (q_{\mathsf{PT}} \mathsf{L}_{\mathsf{PT}})}{\mathsf{L}_{\mathsf{D}}} + \frac{(q_{\mathsf{MS}} \mathsf{L}_{\mathsf{MS}}) + (q_{\mathsf{TMP}} \mathsf{L}_{\mathsf{TMP}}) + (q_{\mathsf{PT}} \mathsf{L}_{\mathsf{PT}})}{\mathsf{L}_{\mathsf{D}}'} \bigg)$$

where BF_D represents the summed BF at the specific bite point; $q_{\rm MS}$, $q_{\rm TMP}$, and $q_{\rm PT}$ represent the PCSA values of the masseter, temporalis, and medial pterygoid, respectively; $L_{\rm MS}$, $L_{\rm TMP}$, and $L_{\rm PT}$ represent lever arm lengths of the masseter, temporalis and medial pterygoid, respectively; $L_{\rm D}$ represents the working-side load arm length of the moment arm for the specific bite point; $L'_{\rm D}$ represents the balancing-side load arm length for the specific bite point; and c represents the force constant of 3 kg/cm².

3.3 | Three-dimensional tooth root analysis

Using Amira 6.3 (Visualization Sciences Group, 2018), all postcanine teeth in the right mandibular quadrant were manually segmented for each specimen except when teeth were damaged, in which case the contralateral side was used. Isolated teeth were converted to surface files (.ply), with an unconstrained smoothing extent of 3 and then exported to Geomagic® Wrap (3D Systems, 2021). Scan and segmentation artifacts in the surface file were then smoothed. Intraobserver error of segmentation and smoothing was found to be less than 1%. Each tooth was then digitally "cut" at the cementoenamel junction in order to separate the tooth root from the tooth crown (Figure 2). Pulp cavities were filled to prevent them from being included in surface area calculations. Surface area was calculated for each isolated tooth root using the Geomagic® Wrap surface area analysis tool.

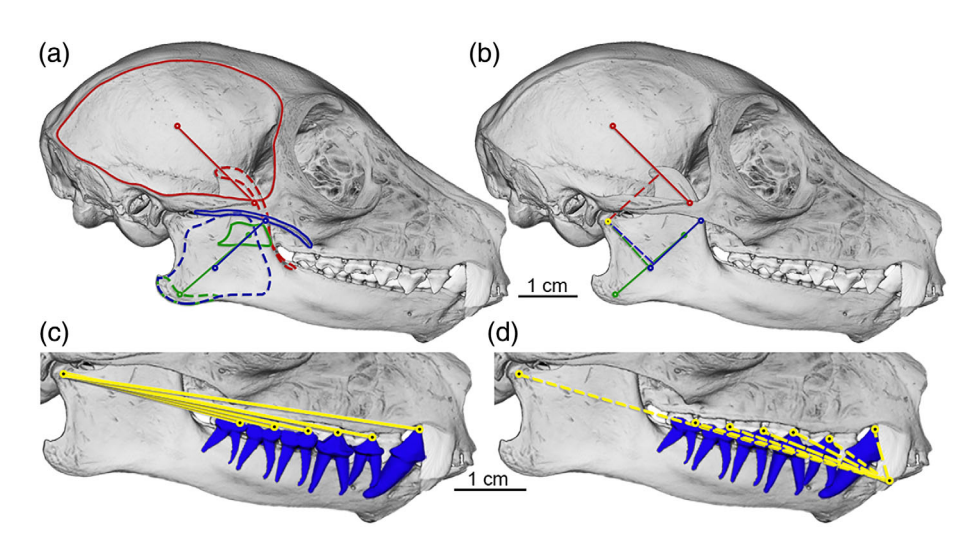


FIGURE 1 Determination of biomechanical variables used for bite force calculation, using lateral photographs of *Eulemur coronatus* (AHR 114035). (a) Temporalis (red), masseter (blue), and medial pterygoid (green) origins (solid outlines), insertions (dashed outlines). Colored circles represent the centroid of each respective muscle origin and insertion. Muscle lines of action represented by a straight line from the centroid of each muscle's origin to the centroid of its insertion (solid line). (b) Muscle moments (dashed lines) measured as the length of a line perpendicular to the muscle's line of action (solid line) to the point of mandibular rotation (yellow circle). (c) Working side bite point leverages (solid yellow line) measured as the distance from the point of rotation to each bite point chosen for this study. (d) Balancing side bite point leverages (dashed yellow line) measured as the distance from the point of rotation to infradentale plus the distance from infradentale to each bite point

3.4 | Dietary categorization

To explore the relationship between TRSA and diet, species were sorted into four dietary categories (Table 1). These include species that consume relatively pliant, unchallenging foods, such as ripe fruits (Category 1), those that consume insects (Category 2), those that consume tough leaves, which require repetitive mastication (Category 3), and those that consume obdurate foods, such as hard fruits, seeds, and nuts (Category 4). Classification was based on published accounts of dietary components (Mittermeier et al., 2012).

3.5 | Size proxies

Because last living body weight was unavailable for specimens in this sample, two different body size proxies were utilized to examine the scaling of TRSA: BM and cranial GM. BM for each specimen was derived from species-specific accounts presented by Mittermeier

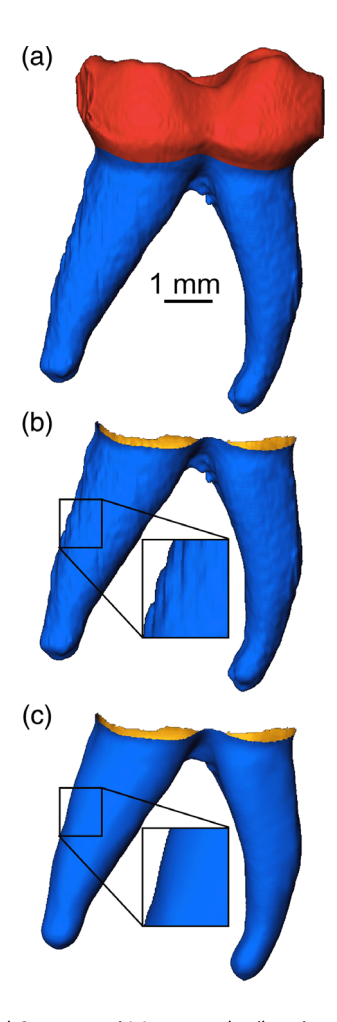


FIGURE 2 (a) Segmented M_2 crown (red) and root (blue) of Eulemur coronatus (AHR 114035). (b) M_2 root (blue) digitally separated from the crown at the cementoenamel junction. (c) M_2 root smoothed to remove scanning and segmentation artifacts. Tooth root surface area measured as smoothed outer surface area (blue), excluding inner surface area (orange)

et al. (2012). Sex-specific BM accounts were used when available. For specimens of unknown sex, overall species averages were used. Cranial GM was calculated from a series of nine measurements (Table 2), each measured from a lateral and superior image of each specimen following the protocol outlined in Hartstone-Rose et al. (2018). The product of these values was taken to the ninth root to produce a GM. Although mandibular length is often used as an additional body size proxy, it has been excluded here because it is so closely related to all of the bite point out-levers and is therefore not a sufficiently independent variable for masticatory biomechanical analysis (Coleman, 2008).

3.6 | Data analysis

All statistical tests used a significance criterion of α < 0.05. All figures were produced in JMP15 Pro (SAS). Although data were collected on Daubentonia madagascariensis, this species, arguably the most derived member of the order (especially in terms of its masticatory anatomy), was included in figures, but because its tooth roots are so categorically different was excluded from all statistical analyses. Prior to analysis, all variables were log transformed and standardized, such that isometry is represented by a slope of 1; three-dimensional variables, such as BM (a product of volume), were reduced to cubic-roots, while two-dimensional variables, such as TRSA and BF (derived from myological cross-sectional areas), were reduced to square-roots. All analyses of TRSA functional correlation were conducted for five different teeth or groupings of teeth: P4, M2, sum of all premolars (P), sum of all molars (M), and total postcanine TRSA (Tot). The individual teeth were chosen for analysis because (with the exception of the previously excluded D. madagascariensis) they are present in all species within the sample. Additionally, P4 represents a transitional tooth (i.e., a key adaptive region between the more caniniform mesial premolars and the generally grinding or pestle-shaped molars), which may have a strong dietary signal (see McGraw & Daegling, 2020 and references therein), and M2 has been used as a representative molar in analyses of diet (e.g., Kay, 1975). The effect of tooth number on each of the tooth category surface area variables (2 vs. 3 for P, 2 vs.

TABLE 2 Measurements that make up the cranial geometric mean

Mandibular length: Posterior edge of the condyle to infradentale

Cranial length: Prosthion to inion

Height of the mandibular corpus: Inferior to M₂ protoconid

Maximum cranial height: Inferior mandible to vertex

Maximum orbital height

Bizygomatic breadth

Maximum cranial breadth: Posterior to the zygomatic arches

Postorbital constriction: Minimum cranial breadth posterior to the orbits

Biorbital width: Maximum width measured on the lateral margins of the orbital walls 3 for M, and 5 vs. 6 for Tot) was assessed using an analysis of variance (ANOVA) as well as comparison of bootstrapped means conducted in R version 4.0.5 (R Core Team, 2021) using randomized sampling with replacement. All iterative tests were conducted with 1000 iterations. Additional analyses of scaling and a comparison of dietary signals across teeth were conducted for each individual tooth.

To study scaling, TRSA variables were regressed on each body size proxy using a model II reduced major axis (RMA) regression to account for uncertainty in both *x*- and *y*-variables. This was repeated for individual higher taxonomic groups (Cercopithecoidea, Platyrrhini, and Strepsirrhini). Residuals from these regressions were used for subsequent analyses as they represent size-adjusted TRSA, or relative TRSA (rTRSA). 95% confidence intervals of bootstrapped slopes for RMA regressions for each of these taxa were compared to determine differences in scaling between taxa. These RMA regressions were produced in R using the package Imodel2 (Legendre, 2018). Additionally, ordinary least squares (OLS) regressions were performed on log transformed TRSA of each individual postcanine tooth against log transformed BM variables to generate fit lines allowing for the prediction of BM from measured TRSA.

ANOVAs were used to assess the differences in rTRSA between dietary categories. This was followed by Tukey post-hoc tests to find statistical differences between individual dietary categories. To assess the relationship between TRSA and BF, residuals from an OLS regression of TRSA against each body size proxy were RMA regressed against residuals from an OLS regression of BF against the same body size proxy. OLS regression was used because deviance in the y-variables (TRSA and BF) was of interest.

To evaluate the potential effects of phylogeny, conventional statistics were run in R followed by phylogenetically adjusted statistics using the packages geiger (Harmon et al., 2008), phytools (Revell, 2012), and ape (Paradis & Schliep, 2019). The phylogenetic branching sequence with dates was obtained from 10kTrees version 3 (Arnold et al., 2010). Conventional ANOVA and phylogenetic ANOVA results were calculated and compared to assess the effects of phylogeny on the relationship between TRSA and diet.

4 | RESULTS

When all tooth category variables were tested, the effect of tooth number on total premolar TRSA and total molar TRSA was found to be statistically significant, such that taxa with more teeth within a given tooth category have a larger TRSA for that category. As such, these tooth category variables were not included in subsequent analyses. All TRSA variables scaled with isometry or positive allometry with one exception; in strepsirrhines, total TRSA scaled with negative allometry against BM (Figure 3; Table 3). Further analysis of differences in scaling were conducted through comparison of bootstrapped 95% confidence intervals of RMA regression slopes. While M₂ TRSA scaled similarly in all taxonomic groups, P₄ TRSA relative to BM scaled significantly differently in strepsirrhines compared to both cercopithecoids and hominoids. Platyrrhine P₄ rTRSA scaling did not

differ significantly from any other lineage. Taxonomic scaling patterns for total postcanine rTRSA were different relative to BM and cranial GM. For total postcanine TRSA relative to both BM and GM, cercopithecoids scaled significantly differently from strepsirrhines; however, relative to GM hominoids also differed significantly from strepsirrhines. These findings were largely contrary to scaling predictions outlined in *Prediction 1*. Due to differences in scaling between these taxonomic groups, rTRSA values for each species were calculated as the residual relative to a taxon-specific RMA regression line. *Tarsius syrichta* TRSA largely fell in line with strepsirrhines of the same body size. *Tarsius syrichta* total TRSA relative to GM fell between strepsirrhine and platyrrhine fit lines. *Tarsius syrichta* P₄ TRSA relative to GM fell in line with platyrrhines rather than strepsirrhines of the same body size.

Using taxon-specific rTRSA for the entire sample, M_2 TRSA relative to GM differed statistically significantly between dietary categories (p=0.02), with a Tukey test revealing significant difference between primates with pliant diets and those with folivorous diets (p=0.01; Figure 4; Table 4). *Hapalemur griseus* has been categorized as a folivore within this dietary scheme; however, bamboo is both hard *and* tough (Amada & Untao, 2001; Lakkad & Patel, 1981). Because *H. griseus* was represented by particularly large residuals (i.e., a functional and statistical outlier), analyses were repeated excluding *H. griseus* (Figure 5). When *H. griseus* was excluded, pairwise comparisons of P_4 and total postcanine TRSA relative to BM also differed between primates with hard diets and those with folivorous diets (p=0.01 and 0.04, respectively; Table 4).

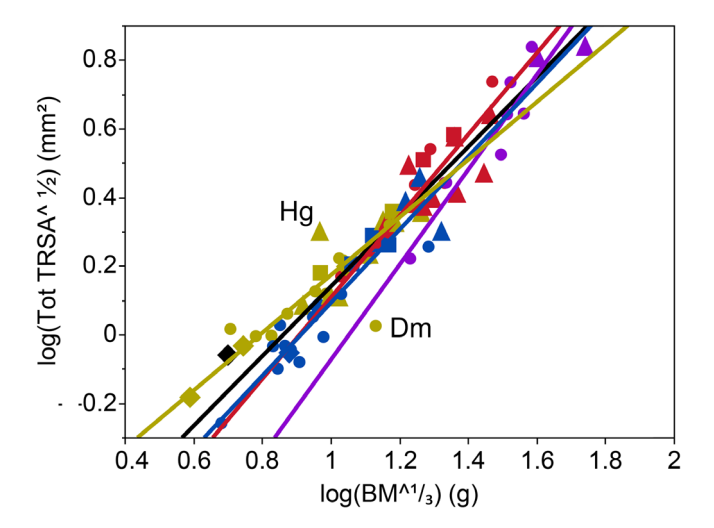


FIGURE 3 Reduced major axis regression lines for whole sample (black) and each taxon individually (Hominoid: Purple, Cercopithecoidea: Red, Platyrrhini: Blue, Strepsirrhini: Yellow, Tarsiidae: Black). Daubentonia madegascariensis (Dm) is shown but excluded for all regression calculations. Hapalemur griseus (Hg) is also indicated (see discussion). Shapes represent dietary categories: Circles represent species with pliant diets, diamonds represent species with insectivorous diets, triangles represent species with folivorous diets, and squares represent species with hard diets

TABLE 3 Descriptive statistics for RMA regressions of TRSA variables against body mass and cranial geometric mean

Body mass proxy Y-variable	Sample	Y-intercept	Slope (β)	Lower β CL	Upper β CL	r ²
P ₄ Root surface area						
Log body mass (g) ^{1/3}	All Primates	-1.28	1.01	0.94	1.08	0.96
	Hominoids	-1.84	1.39	0.96	1.99	0.93
	Cercopithecoids	-1.43	1.14	0.84	1.54	0.74
	Platyrrhines	-1.29	0.99	0.83	1.19	0.88
	Strepsirrhines	-1.05	0.80	0.62	1.04	0.76
Log cranial geometric mean	All Primates	-0.84	1.18*	1.11*	1.16	0.93
	Hominoids	-1.27	1.64*	1.10*	2.45	0.85
	Cercopithecoids	-1.02	1.42*	1.15*	1.75	0.85
	Platyrrhines	-0.85	1.13	0.97	1.31	0.91
	Strepsirrhines	-0.74	1.05	0.88	1.24	0.88
M ₂ Root surface area						
Log body mass (g) ^{1/3}	All Primates	-1.39	1.16	1.07*	1.25	0.95
	Hominoids	-1.71	1.34	0.93	1.94	0.93
	Cercopithecoids	-1.39	1.19	0.86	1.66	0.71
	Platyrrhines	-1.49	1.18	0.96	1.46	0.84
	Strepsirrhines	-1.19	0.99	0.82	1.20	0.86
Log cranial geometric mean	All Primates	-0.89	1.36*	1.25*	1.47	0.89
	Hominoids	-1.15	1.59*	1.07*	2.36	0.85
	Cercopithecoids	-0.96	1.49*	1.20*	1.84	0.84
	Platyrrhines	-0.97	1.34*	1.13*	1.60	0.89
	Strepsirrhines	-0.80	1.30*	1.03*	1.63	0.81
Total postcanine TRSA						
Log body mass (g) ^{1/3}	All Primates	-0.89	1.02	0.95	1.09	0.96
	Hominoids	-1.46	1.39	0.96	1.99	0.93
	Cercopithecoids	-1.08	1.19	0.89	1.58	0.76
	Platyrrhines	-0.98	1.07	0.89	1.27	0.88
	Strepsirrhines	-0.67	0.84*	0.71	0.99*	0.88
Log cranial geometric mean	All Primates	-0.45	1.20*	1.12*	1.28	0.92
	Hominoids	-0.89	1.64*	1.10*	2.44	0.85
	Cercopithecoids	-0.65	1.48*	1.25*	1.76	0.89
	Platyrrhines	-0.51	1.21	1.06	1.38	0.93
	Strepsirrhines	-0.34	1.10	0.94	1.29	0.90

Note: CL represents the 95% confidence interval. r^2 represents the coefficient of determination or the amount of TRSA variation predictable by body size. Abbreviations: RMA, reduced major axis; TRSA, tooth root surface area. *Statistical significance.

When residuals relative to RMA regressions for the whole order were used, only M_2 TRSA relative to GM was statistically significantly different between primates with pliant diets and those with folivorous diets (p=0.01; Table 5). Phylogenetic ANOVA results using whole-order residuals revealed additional statistically significant differences between primates with pliant diets and those with folivorous diets in total postcanine TRSA relative to GM (p=0.04; Table 5). Dietary signals did not change for phylogenetic ANOVA analyses when H. griseus was excluded. These findings partially support $Prediction\ 2$. Additional ANOVAs for individual taxa revealed that dietary differences were

largely driven by strepsirrhines (Table 5). Phylogenetic ANOVA and post-hoc test results are also reported for strepsirrhines and reveal additional dietary signals within the suborder alone (Table 6). Analyses of individual lineages also revealed significant difference between P_4 TRSA relative to GM for cercopithecoids that consume pliant diets and those that consume hard diets (Table 6). This difference remained significant with phylogenetic adjustment. No additional signals were revealed for platyrrhines or hominoids. This is contrary to *Prediction 3*.

Contrary to *Prediction* 4, analysis of differences in taxon-specific rTRSA by dietary category revealed different dietary signals in P_4 and M_2

(Figures 6 and 7; Table 6). Additional analyses of individual postcanine teeth demonstrated a similar pattern across all molars as well as a similar pattern across all premolars when *H. griseus* is excluded (Tables 4 and 7).

Prediction 5 was supported as all RMA regressions of rTRSA against BF had weak correlations. All r^2 values were below 0.07 with a mean of 0.03, such that, independent of body size,

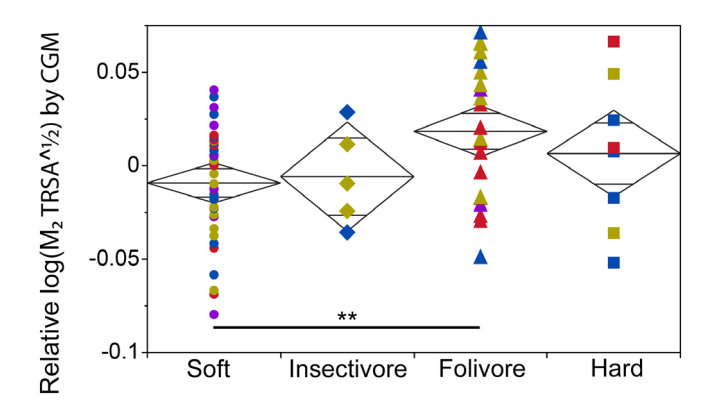


FIGURE 4 Analysis of variance (ANOVA) of M_2 rTRSA by dietary category. Means diamonds represent the 95% confidence interval for each group mean. The center line of each diamond represents the sample mean of each group. Small horizontal lines are "overlap lines"—Marks that indicate statistically significant difference between groups of equal sizes and normal distribution. Because these rules are violated within this sample, these lines should be regarded only as suggestive of significance and not true statistical indications thereof. Line below the diamond plots represents significant difference (*p < 0.05, **p < 0.01, ***p < 0.001) between groups. See Figure 3 caption for symbol color and shape key

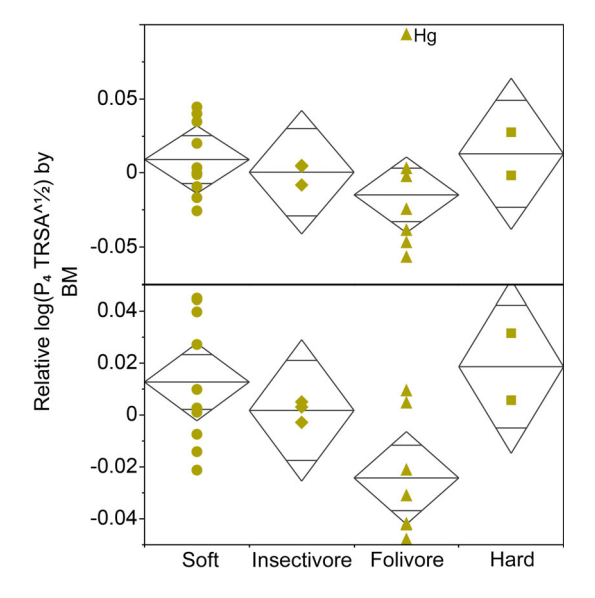


FIGURE 5 Analysis of variance (ANOVA) of strepsirrhine P_4 rTRSA by dietary category including (top) and excluding (bottom) *Hapalemur griseus* (Hg). Lines above the diamond plot represent significant difference (*p < 0.05, **p < 0.01, ***p < 0.001) between groups. See Figure 3 caption for symbol shape key

TABLE 4 ANOVA and Tukey post-hoc test results for taxon-specific tooth root surface area residuals by dietary category

	P ₄ rTRSA by GM	P ₄ rTRSA by BM	M ₂ rTRSA by GM	M ₂ rTRSA by BM	Total postcanine rTRSA by GM	Total postcanine rTRSA by BM
Including H	apalemur					
ANOVA	0.29	0.08	0.02*	0.65	0.12	0.17
Tukey pairv	vise-comparisons					
S to I	0.99	1.00	1.00	1.00	0.97	1.00
S to F	0.60	0.39	0.01*	1.00	0.13	0.64
S to H	0.29	0.35	0.61	0.60	0.35	0.40
I to F	0.98	0.89	0.44	1.00	0.87	0.95
I to H	0.76	0.59	0.91	0.79	0.86	0.64
F to H	0.81	0.05	0.81	0.69	1.00	0.12
Excluding H	apalemur					
ANOVA	0.29	0.02*	0.04*	0.54	0.18	0.07
Tukey pairv	vise-comparisons					
S to I	1.00	1.00	0.99	1.00	0.99	1.00
S to F	0.78	0.14	0.03*	1.00	0.26	0.36
S to H	0.24	0.26	0.63	0.55	0.34	0.33
I to F	0.99	0.74	0.58	1.00	0.91	0.86
I to H	0.69	0.50	0.94	0.75	0.83	0.60
F to H	0.64	0.01*	0.89	0.50	0.98	0.04*

Note: Dietary categories represent: A pliant and mechanically unchallenging diet (soft; S), insectivory (I), folivory (F), and a hard diet (H). Abbreviations: ANOVA, analysis of variance; BM, body mass; GM, geometric mean.

^{*}Statistical significance.

 TABLE 5
 Results of Tukey post-hoc test for whole order TRSA residuals by dietary category with and without phylogenetic adjustment

	P ₄ rTRSA by GM	P ₄ rTRSA by BM	M₂ rTRSA by GM	M₂ rTRSA by BM	Total postcanine rTRSA by GM	Total postcanine rTRSA by BM
Conventio	nal statistics					
S to I	0.72	0.65	0.77	0.57	0.71	0.50
S to F	0.66	0.46	0.01*	0.79	0.10	1.00
S to H	0.66	0.60	0.95	0.80	0.72	0.51
I to F	0.99	0.21	0.68	0.90	0.98	0.47
I to H	1.00	1.00	0.98	0.98	1.00	1.00
F to H	0.99	0.15	0.31	0.99	0.98	0.48
Phylogene	tic adjustment					
S to I	0.52	0.45	0.42	0.35	0.38	0.34
S to F	0.26	0.50	0.00*	0.35	0.04*	0.88
S to H	0.31	0.27	0.50	0.42	0.27	0.21
I to F	0.97	0.32	0.43	0.79	0.69	0.48
I to H	0.98	0.96	0.75	0.73	0.93	0.91
F to H	0.95	0.18	0.16	0.96	0.57	0.41

Note: Dietary categories represent: A pliant and mechanically unchallenging diet (soft; S), insectivory (I), folivory (F), and a hard diet (H). Abbreviations: BM, body mass; GM, geometric mean; TRSA, tooth root surface area.

*Statistical significance.

anatomically derived BF explained less than 7% of the variation in TRSA.

5 | DISCUSSION

Although total postcanine TRSA is not significantly affected by tooth number, tooth number has a significant inverse effect on total premolar TRSA and total molar TRSA. Thus taxa with fewer premolars compensate with larger molar root surface areas and vice versa, such that total postcanine TRSA remains relatively consistent. This may be because, regardless of tooth number, the tooth row as a whole must be capable of resisting masticatory forces. Additionally, postcanine space within the mandible is limited, and there exists a tradeoff between jaw length and mechanical advantage. Taxa with more teeth may need to have smaller teeth in order to fit them within a relatively mechanically efficient jaw.

5.1 | Scaling of TRSA within primates

For the combined sample, all TRSA variables scale with positive allometry or isometry, as has been found for other masticatory force variables (e.g., Deutsch et al., 2020; Hartstone-Rose et al., 2018; Perry, Hartstone-Rose, & Logan, 2011; Perry & Wall, 2008) as well as in a previous study of TRSA scaling in platyrrhines (Perry et al., 2010). This remains true for individual higher taxonomic groups with the exception of total postcanine TRSA relative to BM in strepsirrhines, which scales with negative allometry. Small strepsirrhines have larger total postcanine TRSA than do small haplorhines (Figure 3), while larger

strepsirrhines are similar in TRSA to haplorhines, thus reducing the slope of this line. 95% confidence intervals of bootstrapped y-intercepts for RMA regressed total postcanine TRSA against GM differ significantly between strepsirrhines and haplorhines, suggesting that strepsirrhines have larger TRSAs relative to body size than haplorhines. These findings may relate to the greater prognathism of small strepsirrhines relative to the substantially orthognathic small haplorhines (e.g., the callitrichids), thus giving the former more mesiodistal space, potentially allowing for larger teeth. Alternatively, it may relate to a reduction in canine root volume in the tooth-combed strepsirrhines, giving them more space available for postcanine teeth. Tarsier TRSA aligns with that of strepsirrhines of the same body size, with the exception of P_4 relative to cranial GM, which is more similar to that of platyrrhines of the same skull size.

5.2 | Impacts of diet on TRSA

The largest and most consistent dietary signal within this sample is for folivory versus relatively pliant, unchallenging diets. This split, largely between folivory and frugivory, has been identified in molar crown morphology (e.g., Kay, 1975) as well as in previous studies of platyrrhine TRSA (Perry et al., 2010; Spencer, 2003). This finding is contrary to previous examinations of TRSA in bats (Self, 2015) and carnivorans (Kupczik & Stynder, 2012), which suggest that increased TRSA is largely driven by hard foods rather than tough foods. Within the complete primate sample, a pliant versus tough signal is present in rTRSA-by-GM for each molar (M_1 , M_2 , and M_3). This suggests that molar root morphology has been shaped by the functionally different mechanical demands of tough and soft foods, at least relative to the size of the

 TABLE 6
 ANOVA and Tukey post-hoc test results for taxon-specific tooth root surface area residuals by dietary category for individual taxa

	Analysis and comparison	P ₄ rTRSA by GM	P ₄ rTRSA by BM	M ₂ rTRSA by GM	M ₂ rTRSA by BM	Total postcanine rTRSA by GM	Total postcaning
Hominoids	ANOVA	0.99	0.40	0.71	0.66	0.85	0.52
	Tukey pairwise	-comparisons					
	S to I	_	_	_	_	_	_
	S to F	0.99	0.40	0.71	0.66	0.85	0.52
	S to H	_	_	_	_	_	_
	I to F	_	_	_	_	_	_
	I to H	_	_	_	_	_	_
	F to H	_	_	_	_	_	_
Cercopithecoids	ANOVA	0.02*	0.22	0.10	0.12	0.18	0.14
	Tukey pairwise	-comparisons					
	S to I	_	_	_	_	_	_
	S to F	0.12	0.83	0.67	0.41	0.64	0.30
	S to H	0.03*	0.35	0.08	0.45	0.16	0.67
	I to F	_	_	_	_	_	_
	I to H	_	_	_	_	_	_
	F to H	0.29	0.19	0.19	0.13	0.35	0.19
Cercopithecoids with	ANOVA	0.06	0.46	0.10	0.24	0.36	0.34
phylogenetic adjustment	Tukey pairwise		0.40	0.10	0.24	0.00	0.04
	S to I	_	_	_	_	_	_
	S to F	0.15	0.83	0.91	0.58	0.52	0.55
	S to H	0.13	0.85	0.71	0.06	0.30	0.33
	I to F						
	I to H	_	_	_	_	_	_
		-	-	- 0.10	- 0.17	- 0.15	-
Ole to small the co	F to H	0.20	0.19	0.18	0.17	0.15	0.26
Platyrrhines	ANOVA	0.88	0.58	0.61	0.82	0.89	0.74
	Tukey pairwise	·	4.00	4.00		4.00	
	S to I	0.98	1.00	1.00	0.98	1.00	0.98
	S to F	1.00	1.00	0.62	0.80	0.90	0.97
	S to H	0.92	0.53	0.99	0.97	0.99	0.69
	I to F	0.98	1.00	0.81	0.99	0.92	1.00
	I to H	0.87	0.87	1.00	1.00	0.98	0.97
	F to H	0.98	0.71	0.60	0.97	0.99	0.96
Strepsirrhines	ANOVA	0.90	0.02*	0.01*	0.63	0.10	0.15
	Tukey pairwise	-comparisons					
	S to I	0.98	0.88	0.84	1.00	0.76	0.99
	S to F	1.00	0.02*	0.01*	0.85	0.08	0.33
	S to H	0.93	0.99	0.68	0.75	0.50	0.63
	I to F	0.91	0.36	0.23	0.84	0.81	0.76
	I to H	1.00	0.84	0.98	0.72	0.96	0.62
	F to H	0.92	0.12	0.57	0.96	1.00	0.15
Strepsirrhines with	ANOVA	0.93	0.06	0.05	0.84	0.29	0.32
phylogenetic adjustment	Tukey pairwise	-comparisons					
	S to I	0.61	0.62	0.46	0.90	0.34	0.82
	S to F	0.93	0.02*	0.02*	0.73	0.15	0.32
	S to H	0.65	0.84	0.30	0.18	0.18	0.25
	I to F	0.72	0.23	0.32	0.74	0.72	0.61

(Continues)

TABLE 6 (Continued)

Analysis and comparison	P ₄ rTRSA by GM	P ₄ rTRSA by BM	M ₂ rTRSA by GM	M ₂ rTRSA by BM	Total postcanine rTRSA by GM	Total postcanine rTRSA by BM
I to H	0.98	0.40	0.78	0.23	0.67	0.09
F to H	0.64	0.01*	0.19	0.69	0.84	0.00*

Note: Phylogenetic ANOVA and post-hoc test results are also reported for cercopithecoids and strepsirrhines. Dietary categories represent: A pliant and mechanically unchallenging diet (soft; S), insectivory (I), folivory (F), and a hard diet (H). Dietary categories not represented by specimens are represented by "—." Hapalemur griseus has been excluded from strepsirrhine results.

Abbreviations: ANOVA, analysis of variance; BM, body mass; GM, geometric mean; TRSA, tooth root surface area. *Statistical significance.

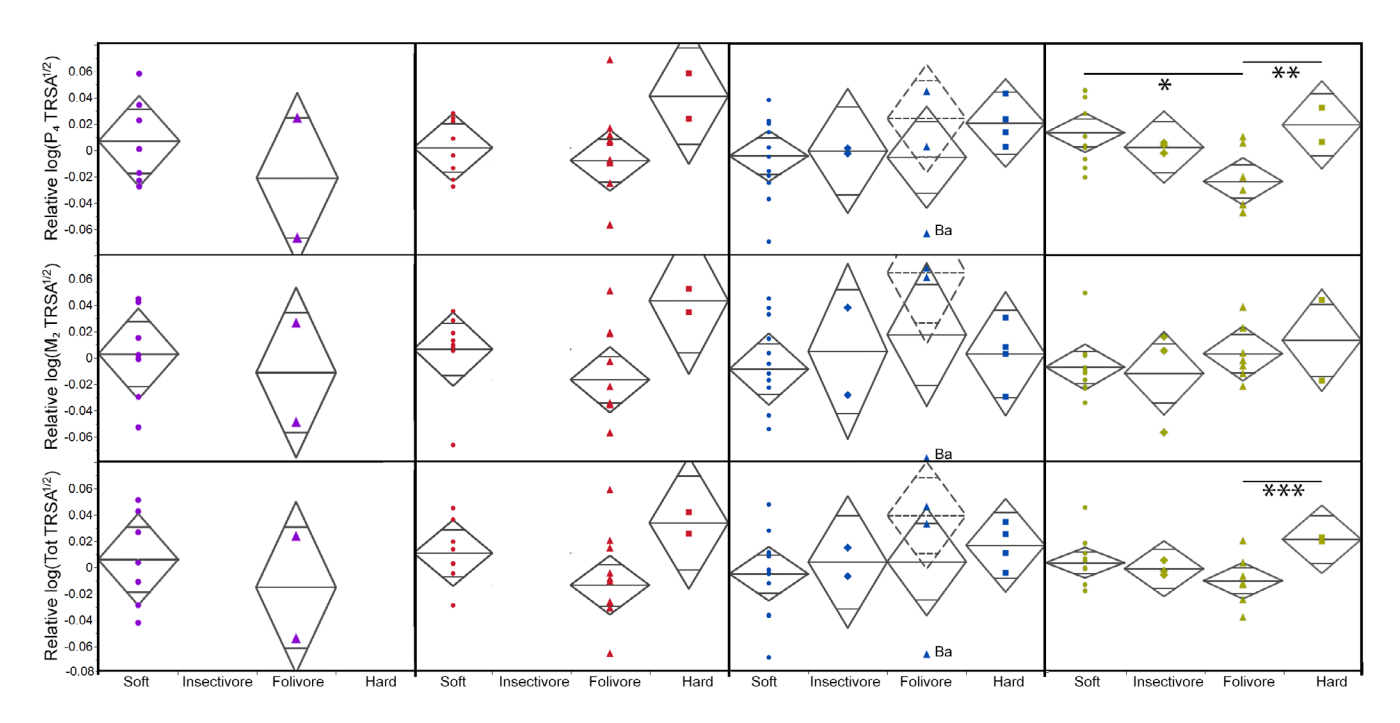


FIGURE 6 Analysis of variance (ANOVA) of TRSA relative to body mass by dietary category for each taxon individually (Hominoidea: Purple, Cercopithecoidea: Red, Platyrrhini: Blue, Strepsirrhini: Yellow). *Hapalemur griseus* has been excluded from analyses. Platyrrhine results are reported with (solid) and without (dashed) *Brachyteles arachnoides* (Ba). Lines above the diamond plot represent significant difference (*p < 0.05, **p < 0.01, ***p < 0.001) between groups. See Figure 3 caption for symbol shape key

skull. Alternatively, tooth root morphology may reflect differences in occlusal morphology, which is highly correlated with diet (e.g., Kay, 1975, 1978). Tooth crown shape may impact the way that masticatory loads are transmitted through the teeth, influencing the loading environment experienced by the roots. A signal for folivory versus a pliant diet is not found relative to BM. While GM and BM are tightly correlated, GM scales with negative allometry relative to BM such that heavier species have relatively smaller skulls. A similar relationship between BM and facial size was previously reported by Scott (2011). This may be because folivory requires a larger gut surface area relative to body size for absorption of nutrients (Chivers & Hladik, 1980). This large gut may impact BM, driving up folivore BM but not GM.

When the sample is analyzed as a whole, premolar signals are absent, potentially because premolars reflect other ingestive and taxonomic differences. However, *H. griseus* is a particularly orthognathic

species, with a molariform P₄, which it likely uses to increase the dental grinding surface. Given this and because its diet of bamboo is so distinct-both tough and hard-H. griseus was removed from the folivorous category resulting in an additional signal for P4 as well as total postcanine TRSA, which may reflect premolar differences. Without H. griseus, an ANOVA of P4 TRSA relative to BM by dietary category becomes significant with the difference being between folivores and species that consume a hard diet (Table 4). This may reflect a functional divide in the usage of P₄ between folivores and hard-object feeders. Whereas folivores largely do not use P4 for grinding, frugivores have been found to use P4 for ingestion and bifurcation of large foods (Hiiemae & Kay, 1972; Perry, 2008; Perry & Hartstone-Rose, 2010; Yamashita, 2003) because of the constraints of gape preventing high linear excursion between the more distal molars. Similarly, hard-object feeders may make use of premolars to consume hard nuts requiring larger gapes than can be accommodated at the more

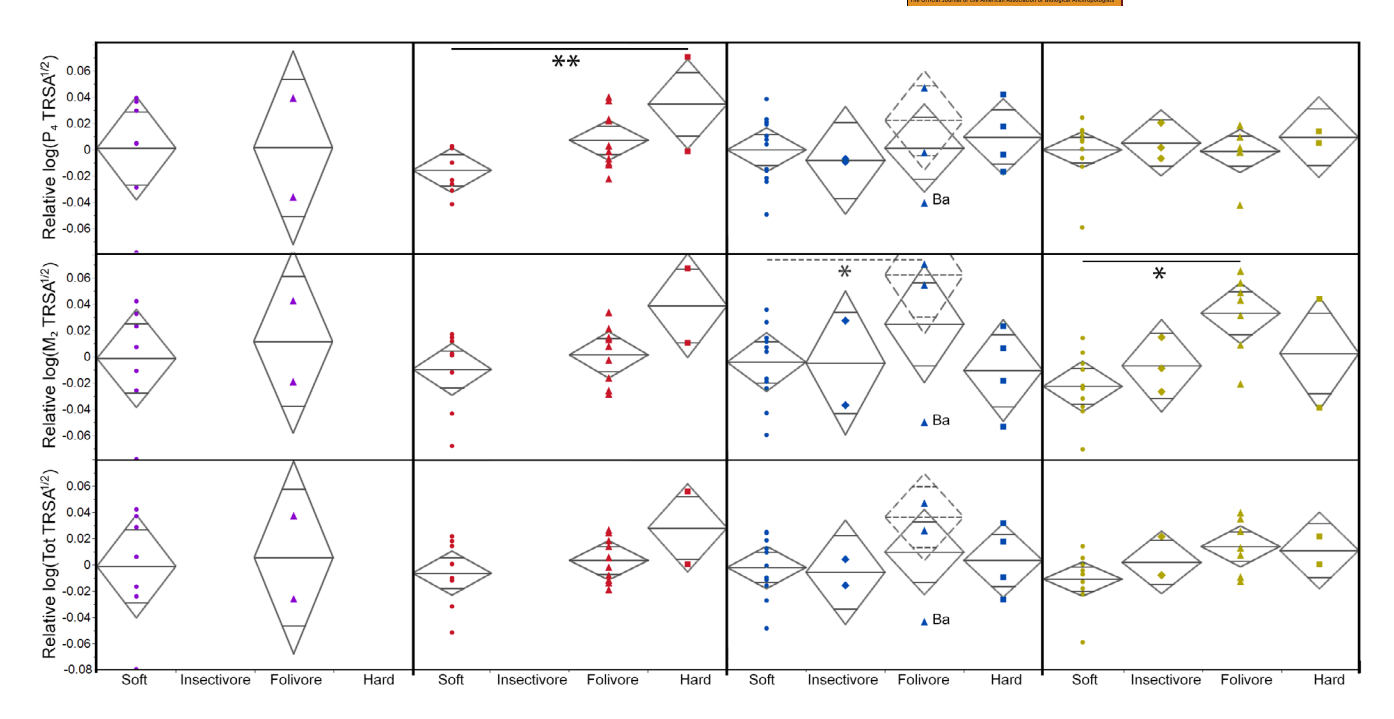


FIGURE 7 Analysis of variance (ANOVA) of TRSA relative to cranial geometric mean by dietary category for each taxon individually (Hominoidea: Purple, Cercopithecoidea: Red, Platyrrhini: Blue, Strepsirrhini: Yellow). *Hapalemur griseus* has been excluded from analyses. Platyrrhine results are reported with (solid) and without (dashed) *Brachyteles arachnoides* (Ba). Lines above the diamond plot represent significant difference (*p < 0.05, **p < 0.01, ***p < 0.001) between groups. See Figure 3 caption for symbol shape key

TABLE 7 ANOVA and Tukey post-hoc test results for taxon-specific tooth root surface area residuals by dietary category

Analysis and comparison	P ₂ rTRSA by GM	P ₂ rTRSA by BM	P ₃ rTRSA by GM	P ₃ rTRSA by BM	M ₁ rTRSA by GM	M ₁ rTRSA by BM	M ₃ rTRSA by GM	M ₃ rTRSA by BM
ANOVA	0.56	0.06	0.70	0.02*	0.04*	0.47	0.06	0.94
Tukey pairwise-com	nparisons							
S to I	0.99	1.00	0.99	1.00	0.92	1.00	0.81	1.00
S to F	0.99	0.35	0.94	0.06	0.03*	1.00	0.04*	0.99
S to H	0.55	0.24	0.65	0.64	0.41	0.44	0.88	0.93
I to F	0.97	0.53	1.00	0.67	0.78	0.99	0.94	1.00
I to H	0.85	0.51	0.95	0.75	0.95	0.82	0.99	1.00
F to H	0.56	0.03*	0.88	0.04*	0.98	0.45	0.65	0.98

Note: Dietary categories represent: A pliant and mechanically unchallenging diet (soft; S), insectivory (I), folivory (F), and a hard diet (H). Abbreviations: ANOVA, analysis of variance; BM, body mass; GM, geometric mean; TRSA, tooth root surface area.

*Statistical significance.

mechanically advantageous molars (see McGraw & Daegling, 2020 and citations therein). This trend was similarly observed across P_2 and P_3 relative to BM (Table 7).

Hard-object feeders do not clearly align with either species that eat tough foods or those that eat pliant foods. This may be because the mastication of tough foods requires frequent chewing cycles (perhaps at high-magnitude forces) with directionally complex loading regimes, while hard food consumption requires larger peak forces but not high frequency forces nor directional complexity, as processing is primarily done through perpendicular crushing (Crompton & Hiiemae, 1970). Tough object mastication may promote more root complexity to prevent tooth displacement (Perry et al., 2010;

Spencer, 2003), potentially through increasing TRSA (although root complexity can also be increased without increasing surface area through elongating root cross-sections or increasing root splay; Kupczik et al., 2018).

5.3 | Impacts of diet on TRSA within Strepsirrhini

Examination of dietary signals within individual higher taxa reveals that these dietary signals are largely driven by strepsirrhine variation. These findings of significance may relate to the sample sizes within the higher taxonomic groups. The sample includes more strepsirrhines

than any other individual higher taxonomic group, while the suborder itself includes fewer species than does Platyrrhini or Cercopithecoidea despite the higher taxonomic level of the former, such that a larger percentage of all strepsirrhine species are represented within this sample. Further, within this sample, strepsirrhines span a larger range of body sizes relative to the maximum body size within the lineage (including members of the smallest genus of the order and the second largest lemur) and dietary categories (i.e., all those found in the order except for the unique obligate faunivory of tarsiers) than any of the other broad lineages. Alternatively, haplorhines may be more anatomically conservative, lacking functional adaptations to diet in tooth roots. This could possibly be a result of generally greater orthognathism within haplorhines placing constraints on the adaptability of their postcanine teeth.

Examination of the strepsirrhine suborder alone further reflects the pattern seen in the whole order analysis: a split between species that consume a pliant, mechanically unchallenging diet and those that consume a primarily folivorous diet (Figure 6). This difference is significant for both P₄ TRSA relative to BM and M₂ TRSA relative to GM. A phylogenetic ANOVA reveals additional signals for difference between pliant and hard-object feeders in P₄ and total postcanine TRSA relative to BM within Strepsirrhini (Table 6; Figure 6). Higher P₄ rTRSA for hard-object feeders may again relate to the constraints of gape at more distal teeth where potential force production is greater. Here, anterior teeth must resist particularly high BFs, potentially requiring larger roots with greater surface areas. Higher total postcanine rTRSA may reflect the need for hard-object feeders to resist higher magnitude forces across the tooth row as a whole compared to species that consume mechanically unchallenging diets.

5.4 | Impacts of diet on TRSA within Platyrrhini

Contrary to previous findings (Perry et al., 2010; Spencer, 2003), no significant differences between dietary categories are found in platyrrhines when this sample is examined as a whole. However, Brachyteles arachnoides rTRSA residuals are particularly low relative to other species within the folivore category. Although several studies suggest that B. arachnoides devotes more than 50% of time spent feeding to leaf consumption, much of this time is devoted to young rather than mature leaf consumption (Milton, 1984; Strier, 1991). Observations by Strier (1991) suggest that B. arachnoides may spend only around 8.86% of foraging time feeding on mature leaves annually. Additionally, more recent observations suggest that B. arachnoides may spend less time feeding on leaves-21.6% of feeding time-with mature leaves making up only 3.5% of total feeding time (Talebi et al., 2005). Because young leaves are significantly less tough than mature leaves (Dunham & Lambert, 2016; Matsuda et al., 2017), processing young leaves may produce a less mechanically challenging loading environment, reducing the need for a large TRSA capable of resisting displacement from complex forces associated with folivory.

When B. arachnoides is removed from the platyrrhine sample, average folivore rTRSA for all tooth categories and body size proxies

become consistently larger than average rTRSA for other dietary categories; however, this relationship is only significant for M2 TRSA relative to GM, with the significant difference being between species with pliant diets and those with folivorous diets (p < 0.05; Figure 7). This potentially suggests that the large TRSA of folivorous platyrrhines is an adaptation to resist displacement from the complex and high frequency forces produced while processing mature leaves; however, significance disappears with phylogenetic correction. The absence of a strong dietary signal may relate to the limitations of this largest but still limited sample—with the exclusion of B. arachnoides, the platyrrhine folivore sample is small (n = 2) and monogeneric. While several folivorous taxa are missing from this sample, the parvorder itself has only two predominantly folivorous genera (Brachyteles and Alouatta), both of which are fairly closely related-within the family Atelidae (Fleagle, 2013). This unbalanced distribution of folivores within Platyrrhini may complicate distinguishing between dietary and phylogenetic signals; however, future studies should attempt to tease apart these factors by incorporating additional taxa within both folivorous genera.

5.5 | Impacts of diet on TRSA within Catarrhini

Among cercopithecoids, no folivory-frugivory signal emerges; however, mean TRSA of hard-object feeders relative to both body size proxies is consistently larger than mean TRSA of species with either folivorous diets or pliant diets for all tooth categories. This relationship is only statistically significant for P4 TRSA relative to GM, with the difference being between species with pliant diets and those with hard diets. Here, the constraints of gape may force hard-object feeders to make greater use of P₄ for crushing obdurate foods, subjecting P₄ to relatively high magnitude forces. As such, P₄ TRSA may need to be large to resist tooth displacement. Average TRSA within Cercopithecoidea was lowest in folivores for all teeth relative to BM. This finding aligns with previous research suggesting that colobine molar crown morphology may reduce the occlusal forces required for processing tough leaves (Kupczik et al., 2009). Similar to observations within Strepsirrhini, however, this pattern was not found relative to GM. This likely reflects the relatively large stomachs of colobines, as colobines display the lowest TRSA values relative to BM.

Although the hominoid sample is too small to yield statistical results, several patterns emerge. As seen in previous examinations of hominoid TRSA relative to a facial size proxy (Kupczik & Dean, 2008), premolar TRSA for *Pongo* is larger than either *P. troglodytes* or *Gorilla* relative to BM. This trend may again reflect the constraints of gape for this primarily frugivorous species that also consumes some hard nuts (Lucas et al., 1994). These foods are potentially too large to be processed at posterior dentition. Relative to GM, however, P₄ rTRSA is smaller than that of the female *G. gorilla*. This pattern suggests that similar to folivorous strepsirrhines and cercopithecoids, *G. gorilla* have relatively large bodies. This relationship between BM and diet across several taxa suggests that while skull size and BM may be adequate body size proxies for the exploration of TRSA scaling and dietary

signals, BM itself is not entirely independent of diet. Contrary to previous examinations of hominoid TRSA relative to a facial size proxy (Kupczik, 2003; Kupczik & Dean, 2008), M2 and total postcanine TRSA of G. gorilla relative to both GM and BM was smaller than or overlapping with that of the substantially frugivorous apes, not matched by similarly larger dentition, as has been observed for their molar crowns (Gingerich et al., 1982). While G. gorilla is often classified as a folivore, observations by Remis et al. (2001) suggest that although the diet of G. gorilla consists primarily of tough plant material during dry seasons, fruit makes up a similar proportion of total nutrition on an annual basis. At least one population of G. gorilla has also been observed feeding on hard-objects seasonally (van Casteren et al., 2019). This dietary diversity may be reflected in TRSA. Future TRSA studies should incorporate data for G. berengei, the most folivorous hominoid (Watts, 1984). In all cases, male G. gorilla TRSA is considerably smaller than that of females, suggesting that the larger BM and skull size of males is not matched by similarly larger dentition. The discrepancy between these and previous observations may relate to the use of different body size proxies or alternatively may be due to individual variation, a problem given the comparatively few hominoid taxa within this sample and in the lineage as a whole.

5.6 | Relationship between BF and TRSA

Relative TRSA correlates poorly with BF; however, BF itself is more strongly correlated with body size than with dietary category (Deutsch et al., 2020; Perry, Hartstone-Rose, & Logan, 2011). While osteological correlates correspond with BF (Perry, 2018) more strongly than does rTRSA, rTRSA seems to better reflect dietary adaptations. While rTRSA does not reflect BF estimates, it may be the case that it does reflect actual physiological BFs; however, in vivo data needed for this examination are absent at this time due to the ethical and methodological challenges posed by its collection. While TRSA may be more useful for dietary reconstruction than is anatomicallyderived BF, this current sample suggests that this may be limited and primarily useful within Strepsirrhini. Individual molar teeth demonstrate clear dietary signals, but only when relative to GM. Skull size is not necessarily available for fossil species (although it is, obviously, more likely to be available than BM). When the highly specialized H. griseus is removed from the sample, P₄ TRSA relative to BM can be used to distinguish folivorous species from either pliant-object feeders or hard-object feeders; however, soft and hard-object feeders cannot be distinguished.

5.7 | Correlation between body size and TRSA

While few strong dietary signals of TRSAs exist for the order Primates as a whole or for individual taxa, strong body size signals exist across nearly all teeth and taxa, with body size explaining most of tooth root variation for each tooth individually (mean $r^2 = 0.82$; maximum $r^2 = 0.92$). Given this tight correlation between TRSA and BM, it seems

that TRSA may be a valuable variable for paleontological BM prediction and reconstruction. The predictive linear equations from OLS regressions of log transformed TRSA and log transformed BM for each tooth by taxon and for the order as a whole are reported in Table 8. The r^2 values for mandibular premolar TRSAs exceed or are similar to those reported previously for two-dimensional measures of tooth crown occlusal area (Gingerich et al., 1982). As such, reconstruction of BM from certain teeth may be more accurate based on root rather than crown surface area. Additionally, while tooth crown surface area can be impacted by dental wear (e.g., Dennis et al., 2004; Ungar et al., 2017; Ungar & Bunn, 2008), TRSA is unimpacted, potentially allowing it to be more widely applicable to the paleontological primate record.

5.8 | Limitations and future directions

This study examines the dietary signals and scaling of mandibular postcanine tooth roots within primates. Due to sampling limitations, most species within this sample are represented by a single individual. As such, this research does not address intraspecific variation. Additionally, some lineage-diet combinations are represented by few specimens and bear further investigation in future research. While force magnitudes experienced by maxillary tooth roots must be identical as loading occurs between the jaws, other factors, such as sinus morphology and force directionality (Dempster et al., 1963), cause splanchnocranium and mandibular corpus morphology to diverge in adulthood (Jung et al., 2021). These differences may independently shape and constrain maxillary tooth root morphology, leading to differences in these patterns relative to those observed or mandibular tooth roots. Future research should explore dietary signals and scaling within maxillary tooth roots independently and as they relate to mandibular tooth root patterns and diet.

Our findings suggest that diet explains relatively little of the variation seen in TRSA for most lineages. The space between the root and alveolar volumes may better reflect dietary signals, as the thickness and distribution of the periodontal ligament play important roles in preventing the tooth from crushing into the alveolar bone (Bemmann et al., 2021). A thicker periodontal ligament and, therefore, larger distance between root and alveolus, could potentially resist highermagnitude forces, better cushioning the tooth and resisting displacement. As such, a stronger signal may exist, distinguishing folivorous species from those that consume hard diets. Future work should explore this potential relationship. Root shape, including splay, in both the mandibular and maxillary teeth is also likely important for fully understanding the relationship between dental morphology and diet.

The absence of correlation between BF and TRSA as well as diet, as observed in previous literature (e.g., Deutsch et al., 2020; Perry, Hartstone-Rose, & Logan, 2011), may suggest that a BF signal does not exist for these variables; however, these findings may alternatively reflect problems with the assumptions and methods of anatomical BF estimation itself. Discrepancies may relate to the way that the complex temporomandibular joint is modeled as a single axis of

Tooth	Sample	Fit line	r²
P_2	All Primates	$\text{log(BM) (g)} = 3.58 + 1.38 \times \text{log(P}_2 \text{ TRSA) (cm}^2\text{)}$	0.70
	Platyrrhines	$\text{log(BM) (g)} = 3.82 + 1.55 \times \text{log(P}_2 \text{TRSA) (cm}^2\text{)}$	0.83
	Strepsirrhines	$\text{log(BM) (g)} = 3.43 + 1.53 \times \text{log(P}_2 \text{TRSA) (cm}^2\text{)}$	0.78
P_3	All Primates	log(BM) (g) $= 3.73 + 1.32 \times \text{log(P}_3 \text{ TRSA)}$ (cm²)	0.91
	Hominoids	$\text{log(BM) (g)} = 4.05 + 0.90 \times \text{log(P}_{3} \text{TRSA) (cm}^2\text{)}$	0.89
	Cercopithecoids	$\text{log(BM) (g)} = 3.73 + 0.94 \times \text{log(P}_3 \text{ TRSA) (cm}^2\text{)}$	0.72
	Platyrrhines	log(BM) (g) $= 3.90 + 1.53 \times \text{log(P}_3 \text{TRSA)}$ (cm²)	0.87
	Strepsirrhines	$\text{log(BM) (g)} = 3.77 + 1.52 \times \text{log(P}_{3} \text{TRSA) (cm}^2)$	0.86
P_4	All Primates	$\text{log(BM) (g)} = 3.77 + 1.42 \times \text{log(P}_{4} \text{ TRSA) (cm}^2\text{)}$	0.91
	Hominoids	$\text{log(BM) (g)} = 4.02 + 1.01 \times \text{log(P}_{\text{4}} \text{ TRSA) (cm}^{\text{2}}\text{)}$	0.87
	Cercopithecoids	$\text{log(BM) (g)} = 3.78 + 1.14 \times \text{log(P}_{\text{4}} \text{ TRSA) (cm}^{\text{2}}\text{)}$	0.74
	Platyrrhines	$\text{log(BM) (g)} = 3.84 + 1.42 \times \text{log(P}_{4} \text{ TRSA) (cm}^{2}\text{)}$	0.88
	Strepsirrhines	$\text{log(BM) (g)} = 3.80 + 1.64 \times \text{log(P}_{\text{4}} \text{ TRSA) (cm}^{\text{2}}\text{)}$	0.77
M_1	All Primates	$\text{log(BM) (g)} = 3.61 + 1.40 \times \text{log(M}_{\text{1}}\text{TRSA) (cm}^2\text{)}$	0.92
	Hominoids	$\text{log(BM) (g)} = 3.90 + 1.05 \times \text{log(M}_{1}\text{TRSA) (cm}^2\text{)}$	0.83
	Cercopithecoids	$\text{log(BM) (g)} = 3.63 + 1.23 \times \text{log(M}_{\text{1}}\text{TRSA) (cm}^2\text{)}$	0.81
	Platyrrhines	$\text{log(BM) (g)} = 3.66 + 1.33 \times \text{log(M}_{\text{1}}\text{TRSA) (cm}^{\text{2}}\text{)}$	0.86
	Strepsirrhines	$\text{log(BM) (g)} = 3.51 + 1.39 \times \text{log(M}_{1}\text{TRSA) (cm}^2\text{)}$	0.86
M_2	All Primates	$\text{log(BM) (g)} = 3.59 + 1.23 \times \text{log(M}_2\text{TRSA) (cm}^2\text{)}$	0.89
	Hominoids	$\text{log(BM) (g)} = 3.88 + 1.04 \times \text{log(M}_2\text{TRSA) (cm}^2\text{)}$	0.87
	Cercopithecoids	$\text{log(BM) (g)} = 3.55 + 1.06 \times \text{log(M}_2\text{TRSA) (cm}^2\text{)}$	0.71
	Platyrrhines	$\text{log(BM) (g)} = 3.71 + 1.16 \times \text{log(M}_2\text{TRSA) (cm}^2\text{)}$	0.84
	Strepsirrhines	$\text{log(BM) (g)} = 3.54 + 1.40 \times \text{log(M}_2\text{TRSA) (cm}^2\text{)}$	0.86
M_3	All Primates	$\text{log(BM) (g)} = 3.69 + 1.19 \times \text{log(M}_{3} \text{TRSA) (cm}^{2}\text{)}$	0.83
	Hominoids	$\text{log(BM) (g)} = 4.02 + 0.97 \times \text{log(M}_3\text{TRSA) (cm}^2\text{)}$	0.83
	Cercopithecoids	$\text{log(BM) (g)} = 3.63 + 0.93 \times \text{log(M}_3\text{TRSA) (cm}^2\text{)}$	0.66
	Platyrrhines	$\text{log(BM) (g)} = 3.82 + 0.93 \times \text{log(M}_3\text{TRSA) (cm}^2\text{)}$	0.64
	Strepsirrhines	$\text{log(BM) (g)} = 3.70 + 1.39 \times \text{log(M}_3\text{TRSA) (cm}^2\text{)}$	0.81

TABLE 8 OLS regression equations for body mass prediction based on TRSA values for the primate order and each taxon individually

Abbreviations: BM, body mass; OLA, ordinary least squares; TRSA, tooth root surface area.

rotation (Terhune et al., 2011) or the use of two-dimensional rather than three-dimensional leverage (Greaves, 1978). As such, it may be the case that anatomically derived BF does reflect actual physiological BFs; however, in vivo data needed to fully examine this correlation are largely absent at this time.

5.9 | Conclusion

The results of this study contribute to the current understanding of trends within tooth root morphology relative to both body size and diet, while representing the most comprehensive examination of TRSA in primates to date. As with previous studies of other masticatory variables within primates, TRSA appears to be more a function of body size than diet across the order and within each lineage. TRSA scales differently across individual tooth variables and lineages; however, all tooth variables scale with positive allometry or isometry relative to both BM and cranial GM, except for strepsirrhine total TRSA

relative to BM, which scales with negative allometry. Like TRSA scaling, dietary signals also vary across individual lineages. While an absence of dietary signals is found within Hominoidea-a finding that runs contrary to previous work within smaller samples (Kupczik, 2003; Kupczik & Dean, 2008)-several statistically significant relationships between TRSA and diet are uncovered within this first examination of TRSA across all major primate clades. For example, there is a distinction between strepsirrhines that consume pliant diets and those that consume folivorous diets as well as between strepsirrhines that consume pliant diets and those that consume hard diets. As in previous examinations of TRSA within Platyrrhini (Perry et al., 2010; Spencer, 2003), a potential signal exists that distinguishes platyrrhines who consume a folivorous diet and those that consume a pliant diet. Additionally, within Cercopithecoidea, a distinction between cercopithecoids that consume pliant diets and those that consume hard diets is uncovered. These signals are all tooth specific and body size proxy specific. Across the sample as a whole, TRSA was poorly correlated with anatomically derived BF, potentially because

anatomically derived BF itself may be poorly correlated with actual in vivo BFs. Nevertheless, these data demonstrate the potential applicability of mandibular postcanine TRSA for the reconstruction of BM in fossil primates (Table 8). In many teeth and taxa, this method of BM reconstruction allows for similar or better accuracy than do methods based on tooth crown surface area (e.g., Gingerich et al., 1982).

ACKNOWLEDGMENTS

We thank Paul Constantino, one anonymous reviewer and two anonymous editors for valuable feedback on an earlier version of this manuscript and Erica Finch for her help with data collection. This publication is Duke Lemur Center publication #1498. Our own scanning was performed at SMIF, a member of the North Carolina Research Triangle Nanotechnology Network (RTNN), which is supported by the National Science Foundation (award number ECCS-2025064) as part of the National Nanotechnology Coordinated Infrastructure (NNCI). Funding was provided by the National Science Foundation IOS-15-57125. We have used data downloaded from the Kyoto University Primate Research Institute's (KUPRI) Digital Morphology Museum and from www.MorphoSource.org, Duke University (funded by DBI-1902242). We also thank the following other researchers for making their CT data available: Eric Delson and the AMNH Department of Mammalogy for providing access to CT data, the collection of which was funded by AMNH and NYCEP. Eric Delson. Kyle Viterbo, and Randall Susman for providing access to CT data, the collection of which was funded by Stony Brook and NYCEP. The Duke Lemur Center for providing access to CT data, originally appearing in Yapuncich et al. (2019), the collection of which was funded by NSF BCS 1540421 to Gabriel S. Yapuncich and Doug M. Boyer. Lauren Gonzales for providing access to CT data, the collection of which was funded by LSB Leakey Foundation. Richard Kay for providing access to CT data, the collection of which was funded by NSF BCS-0090255 and data upload to MorphoSource funded by DBI-1902242. Richard Kay for providing access to CT data, the collection of which was funded by NSF BCS-0851272 and data upload to MorphoSource funded by DBI-1902242. Lynn Lucas and Lynn Copes for providing access to CT data funded by NSF DDIG #0925793 and the Wenner Gren Foundation. James Rossie for providing access to CT data, with data collection funded by NSF BCS-01000825 and data upload to MorphoSource funded by DBI-192242. Tim Rowe for providing access to CT data, with data upload to MorphoSource funded by DBI-1902242.

CONFLICT OF INTEREST

The authors declare no conflict of interest. The funders had no role in the design of the study; in the collection, analyses, or interpretation of data; in the writing of the manuscript, or in the decision to publish the results.

AUTHOR CONTRIBUTIONS

Ashley Deutsch: Conceptualization (lead); data curation (lead); formal analysis (lead); investigation (lead); methodology (lead); project administration (lead); visualization (lead); writing – original draft (lead);

writing – review and editing (equal). Edwin Dickinson: Conceptualization (equal); formal analysis (equal); investigation (supporting); methodology (equal); writing – original draft (supporting); writing – review and editing (equal). Victoria A. Whichard: Formal analysis (equal); writing – original draft (supporting); writing – review and editing (supporting). Giulia R. Lagomarsino: Formal analysis (supporting); writing – original draft (supporting); writing – review and editing (supporting). Jonathan M.G. Perry: Writing – original draft (supporting); writing – original draft (supporting); writing – review and editing (equal). Kornelius Kupczik: Writing – original draft (supporting); writing – review and editing (equal). Adam Hartstone Rose: Conceptualization (supporting); formal analysis (equal); funding acquisition (lead); investigation (equal); resources (lead); software (lead); writing – original draft (supporting); writing – review and editing (equal).

DATA AVAILABILITY STATEMENT

This paper incorporates both CT data publicly available through MorphoSource and novel CT scans collected for the project, which will be made available by the authors at the time of publication (by also uploading to MorphoSource). Any other data are available upon reasonable request.

ORCID

Ashley R. Deutsch https://orcid.org/0000-0002-8535-3280

Edwin Dickinson https://orcid.org/0000-0002-9062-6677

Adam Hartstone-Rose https://orcid.org/0000-0001-5307-5573

REFERENCES

- Amada, S., & Untao, S. (2001). Fracture properties of bamboo. *Composites Part B: Engineering*, 32(5), 451–459. https://doi.org/10.1016/s1359-8368(01)00022-1
- Anapol, F., Shahnoor, N. & Ross, C. F. (2008). Scaling of reduced physiologic cross-sectional area in primate muscles of mastication. In: Chris Vinyard, Matthew J. Ravosa, Christine Wall (Eds.), Primate Craniofacial Function and Biology (pp. 201–216).
- Arnold, C., Matthews, L., & Nunn, C. (2010). The 10kTrees Website: A new online resource for primate phylogeny. Evolutionary Anthropology, 19, 114–118.
- Becerra, F., Echeverría, A., Vassallo, A. I., & Casinos, A. (2011). Bite force and jaw biomechanics in the subterranean rodent Talas tuco-tuco (Ctenomys talarum) (Caviomorpha: Octodontoidea). Canadian Journal of Zoology, 89(4), 334–342. https://doi.org/10.1139/z11-007
- Beertsen, W., McCulloch, C. A., & Sodek, J. (1997). The periodontal ligament: A unique, multifunctional connective tissue. *Periodontology* 2000, 2000(13), 20–40. https://doi.org/10.1111/j.1600-0757.1997. tb00094.x
- Bemmann, M., Schulz-Kornas, E., Hammel, J. U., Hipp, A., Moosmann, J., Herrel, A., Rack, A., Radespiel, U., Zimmermann, E., Kaiser, T. M., & Kupczik, K. (2021). Movement analysis of primate molar teeth under load using synchrotron X-ray microtomography. Journal of Structural Biology, 213(1), 107658. https://doi.org/10.1016/j.jsb.2020.107658
- Boyer, D. M., Gunnell, G. F., Kaufman, S., & McGeary, T. M. (2016). MorphoSource: Archiving and sharing 3-D digital specimen data. *The Pale-ontological Society Papers*, 22, 157–181. https://doi.org/10.1017/scs. 2017.13
- Chivers, D. J., & Hladik, C. M. (1980). Morphology of the gastrointestinal tract in primates: Comparisons with other mammals in relation to diet.

- Journal of Morphology, 166(3), 337–386. https://doi.org/10.1002/imor.1051660306
- Close, R. I. (1972). Dynamic properties of mammalian skeletal muscles. Physiological Reviews, 52(1), 129–197.
- Cobb, S., & Baverstock, H. (2009). Tooth root and craniomandibular morphological integration in the common chimpanzee (*Pan troglodytes*): Alternative developmental models for the determinants of root length. *Frontiers of Oral Biology*, 13, 121–127. https://doi.org/10.1159/000242403
- Coleman, M. N. (2008). What does geometric mean, mean geometrically? Assessing the utility of geometric mean and other size variables in studies of skull allometry. *American Journal of Physical Anthropology*, 135(4), 404–415. https://doi.org/10.1002/ajpa.20761
- Crompton, A., & Hiiemae, K. (1970). Molar occlusion and mandibular movements during occlusion in the American opossum, *Didelphis marsupialis* L. *Zoological Journal of the Linnean Society*, 49(1), 21–47. https://doi.org/10.1111/j.1096-3642.1970.tb00728.x
- Dempster, W. T., Adams, W. J., & Duddles, R. A. (1963). Arrangement in the jaws of the roots of the teeth. *The Journal of the American Dental* Association, 67(6), 779–797. https://doi.org/10.14219/jada.archive. 1963.0364
- Dennis, J. C., Ungar, P. S., Teaford, M. F., & Glander, K. E. (2004). Dental topography and molar wear in *Alouatta palliata* from Costa Rica. *Ameri*can Journal of Physical Anthropology, 125(2), 152–161. https://doi.org/ 10.1002/ajpa.10379
- Deutsch, A. R., Dickinson, E., Leonard, K. C., Pastor, F., Muchlinski, M. N., & Hartstone-Rose, A. (2020). Scaling of anatomically derived maximal bite force in primates. *The Anatomical Record*, 303(7), 2026–2035. https://doi.org/10.1002/ar.24284
- Dunham, N. T., & Lambert, A. L. (2016). The role of leaf toughness on foraging efficiency in Angola black and white colobus monkeys (Colobus angolensis palliatus). American Journal of Physical Anthropology, 161(2), 343–354. https://doi.org/10.1002/ajpa.23036
- Eng, C. M., Ward, S. R., Vinyard, C. J., & Taylor, A. B. (2009). The morphology of the masticatory apparatus facilitates muscle force production at wide jaw gapes in tree-gouging common marmosets (*Callithrix jacchus*). *The Journal of Experimental Biology*, 212(Pt 24), 4040–4055. https://doi.org/10.1242/jeb.029983
- Fleagle, J. G. (2013). Primate adaptation and evolution (3rd ed.). Elsevier Inc. Gans, C. (1982). Fiber architecture and muscle function. Exercercise and Sport Sciences Reviews, 10, 160–207.
- Gans, C., & Bock, W. J. (1965). The functional significance of muscle architecture—A theoretical analysis. Ergebnisse der Anatomie und Entwicklungsgeschichte, 38, 115–142.
- Gingerich, P. D., Smith, B. H., & Rosenberg, K. (1982). Allometric scaling in the dentition of primates and prediction of body weight from tooth size in fossils. American Journal of Physical Anthropology, 58(1), 81–100. https://doi.org/10.1002/ajpa.1330580110
- Greaves, W. S. (1978). The jaw lever system in ungulates: A new model. Journal of Zoology, 184, 271–285.
- Greaves, W. S. (1983). A functional analysis of carnassial biting. *Biological Journal of the Linnean Society*, 20(4), 353–363. https://doi.org/10.1111/j.1095-8312.1983.tb01596.x
- Greaves, W. S. (2012). The mammalian jaw: A mechanical analysis. Cambridge University Press.
- Harmon, L., Weir, J., Brock, C., Glor, R., & Challenger, W. (2008). GEIGER: Investigating evolutionary radiations. *Bioinformatics*, 24, 129–131.
- Hartstone-Rose, A., Deutsch, A. R., Leischner, C. L., & Pastor, F. (2018). Dietary correlates of masticatory muscle fiber architecture in primates. *The Anatatomical Record*, 301, 311–324.
- Hartstone-Rose, A., Dickinson, E., Deutsch, A. R., Worden, N., & Hirschkorn, G. A. (2021). Masticatory muscle architectural correlates of dietary diversity in Canidae, Ursidae, and across the order Carnivora. The Anatomical Record. Online.

- Hartstone-Rose, A., Hertzig, I., & Dickinson, E. (2019). Bite force and masticatory muscle architecture adaptations in the dietarily diverse Musteloidea (Carnivora). The Anatomical Record, 302(12), 2287–2299.
- Hartstone-Rose, A., Perry, J. M. G., & Morrow, C. J. (2012). Bite force estimation and the fiber architecture of felid masticatory muscles. *The Anatomical Record*, 295(8), 1336–1351. https://doi.org/10.1002/ar. 22518
- Hiiemae, K., & Kay, R. F. (1972). Trends in the evolution of primate mastication. *Nature*, 240(5382), 486–487. https://doi.org/10.1038/240486a0
- Hylander, W. L., Johnson, K. R., & Crompton, A. W. (1987). Loading patterns and jaw movements during mastication in *Macaca fascicularis*: A bone-strain, electromyographic, and cineradiographic analysis. *American Journal of Physical Anthropology*, 72(3), 287–314. https://doi.org/10.1002/ajpa.1330720304
- Jung, H., Simons, E., & von Cramon-Taubadel, N. (2021). Ontogenetic changes in magnitudes of integration in the macaque skull. American Journal of Physical Anthropology, 174, 76–88.
- Kay, R. F. (1975). The functional adaptations of primate molar teeth. American Journal of Physical Anthropology, 43(2), 195–215. https://doi. org/10.1002/ajpa.1330430207
- Kay, R. F. (1978). Molar structure and diet in extant Cercopithecidae. In P. M. Butler & K. A. Joysey (Eds.), Development, function and evolution of teeth (pp. 309–339). Academic.
- Kovacs, I. (1971). A systematic description of dental roots. In A. A. Dahlberg (Ed.), *Dental morphology and evolution* (pp. 211–256). The University of Chicago.
- Kovacs, I. (1979). The surface characteristics of tooth roots and their biomechanical importance. OSSA International Journal of Skeletal Research, 6, 181–192.
- Kupczik, K. (2003). Tooth root morphology in primates and carnivores (PhD dissertation; University College London).
- Kupczik, K., & Dean, M. C. (2008). Comparative observations on the tooth root morphology of Gigantopithecus blacki. Journal of Human Evolution, 54(2), 196–204.
- Kupczik, K., & Hublin, J.-J. (2010). Mandibular molar root morphology in Neanderthals and Late Pleistocene and recent Homo sapiens. Journal of Human Evolution, 59(5), 525–541.
- Kupczik, K., Olejniczak, A. J., Skinner, M. M., & Hublin, J. J. (2009). Molar crown and root size relationship in anthropoid primates. Frontiers in Oral Biology, 13, 16–22. https://doi.org/10.1159/000242384
- Kupczik, K., & Stynder, D. (2012). Tooth root morphology as an indicator for dietary specialization in carnivores (Mammalia: Carnivora). *Biologi*cal Journal of the Linnean Society, 105(2), 456–471. https://doi.org/10. 1111/j.1095-8312.2011.01779.x
- Kupczik, K., Toro-Ibacache, V., & Macho, G. A. (2018). On the relationship between maxillary molar root shape and jaw kinematics in Australopithecus africanus and Paranthropus robustus. Royal Society Open Science, 5(8), 180825. https://doi.org/10.1098/rsos. 180825
- Laird, M. F., Granatosky, M. C., Taylor, A. B., & Ross, C. F. (2020). Muscle architecture dynamics modulate performance of the superficial anterior temporalis muscle during chewing in capuchins. *Scientific Reports*, 10(1), 1–13. https://doi.org/10.1038/s41598-020-63376-y
- Lakkad, S. C., & Patel, J. M. (1981). Mechanical properties of bamboo, a natural composite. Fibre Science and Technology, 14(4), 319–322. https://doi.org/10.1016/0015-0568(81)90023-3
- Legendre, P. (2018). Imodel2: Model II Regression. Retrieved from https:// CRAN.R-project.org/package=Imodel2 R package version 1.7-3.
- Leigh, S. R. (1994). Relations between captive and noncaptive weights in anthropoid primates. Zoo Biology, 13(1), 21–43. https://doi.org/10. 1002/zoo.1430130105
- Leonard, K. C., Worden, N., Boettcher, M. L., Dickinson, E., & Hartstone-Rose, A. (2021a). Effects of freezing and short-term fixation on muscle

- mass, volume, and density. *The Anatomical Record. Online*, 1–10. https://doi.org/10.1002/ar.24639
- Leonard, K. C., Worden, N., Boettcher, M. L., Dickinson, E., & Hartstone-Rose, A. (2021b). Effects of long-term ethanol storage on muscle architecture. The Anatomical Record. Online, 1–15. https://doi.org/10.1002/ar.24638
- Leonard, K. C., Worden, N., Boettcher, M. L., Dickinson, E., Omstead, K. M., Burrows, A. M., & Hartstone-Rose, A. (2021). Anatomical and ontogenetic influences on muscle density. *Scientific Reports*, 11(1), 2114. https://doi.org/10.1038/s41598-021-81489-w
- Lieber, R. L. (1986). Skeletal muscle adaptability. I: Review of basic properties. *Development Medicine & Child Neurology*, 28, 390–397.
- Lieber, R. L., & Fridén, J. (2000). Functional and clinical significance of skeletal muscle architecture. Muscle & Nerve, 23(11), 1647–1666.
- Lieber, R. L., & Ward, S. R. (2011). Skeletal muscle design to meet functional demands. Philosophical Transactions of the Royal Society of London B, 366(1570), 1466–1476.
- Lucas, P. W., Peters, C. R., & Arrandale, S. R. (1994). Seed-breaking forces exerted by orang-utans with their teeth in captivity and a new technique for estimating forces produced in the wild. *American Journal of Physical Anthropology*, 94(3), 365–378. https://doi.org/10.1002/ajpa. 1330940306
- Matsuda, I., Clauss, M., Tuuga, A., Sugau, J., Hanya, G., Yumoto, T., Bernard, H., & Hummel, J. (2017). Factors affecting leaf selection by foregut-fermenting proboscis monkeys: New insight from in vitro digestibility and toughness of leaves. *Scientific Reports*, 7(1), 42774. https://doi.org/10.1038/srep42774
- McGraw, W. S., & Daegling, D. J. (2020). Diet, feeding behavior, and jaw architecture of Taï monkeys: Congruence and chaos in the realm of functional morphology. Evolutionary Anthropology: Issues, News, and Reviews, 29(1), 14–28. https://doi.org/10.1002/evan.21799
- Milton, K. (1984). Habitat, diet, and activity patterns of free-ranging woolly spider monkeys (*Brachyteles arachnoides* E. Geoffroy 1806). *Interna*tional Journal of Primatology, 5(5), 491–514. https://doi.org/10.1007/ bf02692271
- Mittermeier, R., Rylands, A., & Wilson, D. (2012). Handbook of the mammals of the world: Primates (Vol. 3). Barcelona, Spain: Lynx Edicions.
- Paradis, E., & Schliep, K. (2019). ape 5.0: An environment for modern phylogenetics and evolutionary analyses in R. Bioinformatics, 35, 526–528.
- Perry, J. M. G. (2008). Anatomy of mastication in extant strepsirrhines and Eocene adapines (PhD dissertation). Duke University
- Perry, J. M. G. (2018). Inferring the diets of extinct giant lemurs from osteological correlates of muscle dimensions. *Anatomical Record (Hoboken)*, 301(2), 343–362. https://doi.org/10.1002/ar.23719
- Perry, J. M. G., & Hartstone-Rose, A. (2010). Maximum ingested food size in captive strepsirrhine primates: Scaling and the effects of diet. American Journal of Physical Anthropology, 142(4), 625–635. https://doi.org/10.1002/ajpa.21285
- Perry, J. M. G., Hartstone-Rose, A., & Logan, R. L. (2011). The jaw adductor resultant and estimated bite force in primates. *Anatomy Research International*, 2011, 929848. https://doi.org/10.1155/2011/929848
- Perry, J. M. G., Hartstone-Rose, A., & Wall, C. E. (2011). The jaw adductors of strepsirrhines in relation to body size, diet, and ingested food size. Anatatomical Record, 294(4), 712–728. https://doi.org/10.1002/ar. 21354
- Perry, J. M. G., Kay, R. F., Vizcaíno, S. F., & Bargo, M. S. (2010). Tooth root size, chewing muscle leverage, and the biology of *Homunculus patagonicus* (Primates) from the late early Miocene of Patagonia. *Ameghiniana*, 47(3), 355–371.
- Perry, J. M. G., Macneill, K. E., Heckler, A. L., Rakotoarisoa, G., & Hartstone-Rose, A. (2014). Anatomy and adaptations of the chewing muscles in *Daubentonia* (Lemuriformes). *Comparative Study*, 297(2), 308–316. https://doi.org/10.1002/ar.22844

- Perry, J. M. G., & Wall, C. E. (2008). Scaling of the chewing muscles in Prosimians. In C. Vinyard, M. J. Ravosa, & C. Wall (Eds.), *Primate craniofacial function and biology* (pp. 217–240). Springer US.
- R Core Team. (2021). R: A language and environment for statistical computing. R Foundation for Statistical Computing, . Retrieved from https:// www.R-project.org/
- Radinsky, L. B. (1981). Evolution of skull shape in carnivores, 2: Additional modern carnivores. *Biological Journal of the Linnaean Society*, 16(4), 337–355
- Remis, M. J., Dierenfeld, E. S., Mowry, C. B., & Carroll, R. W. (2001). Nutritional aspects of Western lowland gorilla (*Gorilla gorilla gorilla*) diet during seasons of fruit scarcity at Bai Hokou, Central African Republic. *International Journal of Primatology*, 22(5), 807–836. https://doi.org/10.1023/a:1012021617737
- Revell, L. (2012). phytools: An R package for phylogenetic comparative biology (and other things). Methods in Ecology and Evolution, 3, 217–223.
- Rosenberger, A. L. (1992). Evolution of feeding niches in New World monkeys. American Journal of Physical Anthropology, 88(4), 525–562. https://doi.org/10.1002/ajpa.1330880408
- Rosenberger, A. L., & Kinzey, W. G. (1976). Functional patterns of molar occlusion in platyrrhine primates. *American Journal of Physical Anthropology*, 45(2), 281–298. https://doi.org/10.1002/ajpa.1330450214
- Rueden, C. T., Schindelin, J., Hiner, M. C., DeZonia, B. E., Walter, A. E., Arena, E. T., & Eliceiri, K. W. (2017). ImageJ2: ImageJ for the next generation of scientific image data. *BMC Bioinformatics*, 18(1), 529. https://doi.org/10.1186/s12859-017-1934-z
- Schumacher, G. H. (1961). Funktionelle Morphologie der Kaumuskulatur. Gustav Fischer.
- Scott, J. E. (2011). Folivory, frugivory, and postcanine size in the cercopithecoidea revisited. American Journal of Physical Anthropology, 146(1), 20–27. https://doi.org/10.1002/ajpa.21535
- Self, C. J. (2015). Dental root size in bats with diets of different hardness. *Journal of Morphology*, 276(9), 1065–1074.
- Siciliano-Martina, L., Light, J. E., & Lawing, A. M. (2021). Cranial morphology of captive mammals: A meta-analysis. Frontiers in Zoology, 18(1), 4. https://doi.org/10.1186/s12983-021-00386-0
- Spencer, M. A. (1998). Force production in the primate masticatory system: Electromyographic tests of biomechanical hypotheses. *Journal of Human Evolution*, 34(1), 25–54. https://doi.org/10.1006/jhev.1997.0180
- Spencer, M. A. (1999). Constraints on masticatory system evolution in anthropoid primates. American Journal of Physical Anthropology, 108, 483–506.
- Spencer, M. A. (2003). Tooth-root form and function in platyrrhine seedeaters. American Journal of Physical Anthropology, 122(4), 325–335. https://doi.org/10.1002/ajpa.10288
- Strier, K. B. (1991). Diet in one group of woolly spider monkeys, or muriquis (Brachyteles arachnoides). American Journal of Primatology, 23(2), 113–126. https://doi.org/10.1002/ajp.1350230205
- Talebi, M., Bastos, A., & Lee, P. C. (2005). Diet of southern muriquis in continuous Brazilian Atlantic Forest. *International Journal of Primatology*, 26(5), 1175–1187. https://doi.org/10.1007/s10764-005-6463-3
- Taylor, A. B., & Vinyard, C. J. (2009). Jaw-muscle fiber architecture in tufted capuchins favors generating relatively large muscle forces without compromising jaw gape. *Journal of Human Evolution*, 57(6), 710–720. https://doi.org/10.1016/j.jhevol.2009.06.001
- Taylor, A. B., & Vinyard, C. J. (2013). The relationships among jaw-muscle fiber architecture, jaw morphology, and feeding behavior in extant apes and modern humans. *American Journal of Physical Anthropology*, 151(1), 120–134. https://doi.org/10.1002/ajpa.22260
- Terhune, C. E., Iriarte-Diaz, J., Taylor, A. B., & Ross, C. F. (2011). The instantaneous center of rotation of the mandible in nonhuman primates. *Integrative and Comparative Biology*, 51(2), 320–332. https:// doi.org/10.1093/icb/icr031

- Ungar, P. S., & Bunn, J. M. (2008). Primate dental topographic analysis and functional morphology. In G. C. Nelson & J. D. Irish (Eds.), *Technique* and application in dental anthropology (pp. 253–265). Cambridge University Press.
- Ungar, P. S., Hartgrove, C. L., Wimberly, A. N., & Teaford, M. F. (2017). Dental topography and microwear texture in *Sapajus apella*. *Biosurface and Biotribology*, 3(4), 124–134. https://doi.org/10.1016/j.bsbt.2017. 12.002
- van Casteren, A., Wright, E., Kupczik, K., & Robbins, M. M. (2019). Unexpected hard-object feeding in Western lowland gorillas. *American Journal of Physical Anthropology*, 170(3), 433–438. https://doi.org/10.1002/ajpa.23911
- Vinyard, C. J., Wall, C. E., Williams, S. H., & Hylander, W. L. (2008). Patterns of variation across primates in jaw-muscle electromyography during mastication. *Integrative and Comparative Biology*, 48(2), 294–311. https://doi.org/10.1093/icb/icn071
- Watts, D. P. (1984). Composition and variability of mountain gorilla diets in the Central Virungas. American Journal of Primatology, 7(4), 323–356. https://doi.org/10.1002/ajp.1350070403
- Winchester, J. M., Boyer, D. M., St. Clair, E. M., Gosselin-Ildari, A. D., Cooke, S. B., & Ledogar, J. A. (2014). Dental topography of platyrrhines and prosimians: Convergence and contrasts. American Journal of Physical Anthropology, 153(1), 29–44. https://doi.org/10.1002/ajpa.22398

- Wood, B., Abbott, S., & Uytterschaut, H. (1988). Analysis of the dental morphology of Plio-Pleistocene hominids. IV. Mandibular postcanine root morphology. *Journal of Anatomy*, 156, 107.
- Yamashita, N. (2003). Food procurement and tooth use in two sympatric lemur species. *American Journal of Physical Anthropology*, 121(2), 125–133. https://doi.org/10.1002/ajpa.10206
- Yapuncich, G. S., Kemp, A. D., Griffith, D. M., Gladman, J. T., Ehmke, E., & Boyer, D. M. (2019). A digital collection of rare and endangered lemurs and other primates from the Duke Lemur Center. *PLoS One*, 14(11), e0219411. https://doi.org/10.1371/journal.pone. 0219411

How to cite this article: Deutsch, A. R., Dickinson, E., Whichard, V. A., Lagomarsino, G. R., Perry, J. M. G., Kupczik, K., & Hartstone-Rose, A. (2022). Primate body mass and dietary correlates of tooth root surface area. *American Journal of Biological Anthropology*, 177(1), 4–26. https://doi.org/10.1002/ajpa.24430